Adaptive Inter-Loop Aiding for Performance Improvements in Low CNIR Environments

Faisal Khan, Andrew Dempster and Chris Rizos, *University of New South Wales*

Abstract

Use of loop aiding for facilitating the operation of Global Positioning System (GPS) receivers in low Carrier-to-Noise and Interference (CNIR) environments has been widely researched in recent years. Locata, a terrestrial radio navigation system working on similar principles as GPS, can also make use of loop aiding techniques with some additional advantages. Locata employs dual-frequency and dual-antenna transceivers (LocataLites) allowing a Locata rover receiver to track four signals from each LocataLite. This paper proposes that the carrier tracking loops used for tracking these signals can adaptively aid each other to maintain lock in low CNIR environments. Performance of this proposed scheme is evaluated and an analytical description and test results are presented. Results show that the loop aiding scheme allows potential reduction of the tracking loop bandwidth down to 0.5Hz, enabling it to track signals with CNIR as low as 21.5dB-Hz. A relationship between the aided loop's performance and the quality of the signal tracked by the aiding loop is also developed and analysed. It is identified that any degradation in the quality of the signal tracked by the aiding loop can affect the aided loop's performance. Use of Adaptive Kalman filtering is suggested as a possible solution to this problem and improves the situation by a further 2.5dB-Hz. Using an analytical approach, it is also shown that a lower bound on the aided loop's expected performance is predictable. It is also established that, by using inter-loop aiding, the Locata system gains more than similarly aided GPS receivers.

Index Terms

Tracking loops, Loop aiding, Phase jitter, Adaptive Kalman filtering.

Faisal Khan, Andrew Dempster and Chris Rizos are with School of Surveying and Spatial Information Systems, University of New South Wales, Australia. Emails: faisal@student.unsw.edu.au, a.dempster@unsw.edu.au, c.rizos@unsw.edu.au

Adaptive Inter-Loop Aiding for Performance Improvements in Low CNIR Environments

I. INTRODUCTION

Operation of Global Navigation Satellite Systems (GNSS) in classically difficult positioning environments has been an issue, particularly with regard to weak received signal levels, poor geometry conditions, and continuously changing multipath scenarios. Locata Corporation's Locata Positioning Network aims to address performance degradation in such situations. A Locata Network (LocataNet) is comprised of time-synchronised terrestrial transceivers (called LocataLites), operating in the 2.4GHz ISM band and transmitting signals appropriate for positioning. Use of time-synchronised transmitters allows single point positioning with centimetre level accuracy. Operation in the ISM band permits signal reception at much higher power levels than those received from GPS, and avoids any licence requirement. This makes the system feasible for deployment in many situations and environments. However, operation in the licence-free ISM band is vulnerable to RF interference (RFI) from various other devices using the same spectral band. Interference from these devices artificially elevates the noise floor, degrading Locata signal's carrier-to-noise and interference ratio (CNIR). Therefore reception of Locata signals requires that special attention be paid to interference rejection/mitigation for optimal operation. There have been some improvements in Locata's interference rejection capabilities in the current version (V3R4). However, it was identified in the authors' previous work [1] that received RFI can cause Locata to operate sub-optimally. In [1], it was identified that some inherent characteristics of the Locata network can be exploited to gain further improvements in terms of noise and interference mitigation. In this paper the authors propose a carrier loop aiding scheme which enables Locata to track signals with CNIR reduced by noise, unintentional interference and/or jamming.

The concept of Doppler aiding using either external aids, e.g. from Inertial Navigation Systems (INS)) or internal aids (from another tracking loop), is not new. Advantages of aiding have been analysed and explored in both theory and practice [2], [3]. Such concepts can be applied to any radio navigation system, and Locata is no exception. However, the Locata system architecture allows some unique advantages to be gained from this concept. This is mainly because Locata uses dual-antenna transceivers (LocataLites) with each antenna transmitting signals at two different frequencies. In GPS, currently a maximum of two signals (L1 and L2) are available from all satellites, with L2 tracking only available in high-end surveying/geodesy receivers. Usually, the fully civilian-accessible L1 has been used to aid L2, as the L1 carrier loop provided more accurate estimates of the received signal dynamics

[4]. If this aiding signal is corrupted due to received interference at the L1 frequency, the advantages of aiding are lost. With the introduction of the new L2C signal, the dataless channel of L2 becomes a better choice to be used as an aiding signal in terms of sensitivity and reliability (as offered by an increased linearity region and lower carrier frequency) [5]. However, the situation would remain unchanged if the interference occurs at the L2 frequency. For Locata, the availability of two carriers for tracking at each of the two frequencies (referred to here as S1 and S6), offers a solution to this problem. It is likely that both carriers will be differently affected by the received interference. A possible situation could be when a nearby WiFi network, operating in the 2.4GHz ISM band, uses a channel which is in a co-frequency situation with the one of the Locata carriers. Availability of two carrier tracking loops (corresponding to two separate spreading codes on separate antennas) at each of the carrier frequencies permits one to keep one carrier loop from each frequency as an aiding loop and the other as the aided loop. In the case where interference is received at either or both of the two frequencies, the less affected of the two aiding loops can provide signal dynamics estimates to both aided carrier loops at two different frequencies. This permits relatively cleaner measurements from the aided loops at both the frequencies even if one or both of the two frequencies are affected by received noise and interference. This is the kernel of the loop-aiding scheme proposed in this paper. This paper analyses this scheme using simulations and suggests a relationship between the aided loop's total phase jitter and the quality of the signal tracked by the aiding loop. It is also recognised here that the aiding loop can also contribute to the noise in the aided loop. Use of Adaptive Kalman Filtering is suggested as a possible solution for performance improvement in such situations. It is discussed, and shown through simulations, that Adaptive Kalman Filter reduces the noise in the carrier loop's output without making it vulnerable to signal dynamics.

The remainder of the paper is organised as follows. After introducing the concepts in Section 1, Section 2 discusses the basics of loop aiding and identifies the problems associated with not using loop aiding. Section 3 proposes the solution and presents the details of the proposed method. Section 4 identifies that a lower bound is predictable on the expected performance of the aided loop. Section 5 discusses the simulations performed to test the tracking loop's performance before and after implementation of this method and analyses the results. This is followed, in Section 6, by a proposed augmentation based on Adaptive Kalman filtering for further noise reduction. Section 7 concludes the paper.

II. Loop Aiding

Carrier phase positioning is the main mode of operation for Locata. Therefore the quality of carrier phase measurements originating from the carrier tracking loops (CTL) dictates the quality of the final position solution.

Nevertheless, CTL has been identified as the weakest link in a positioning receiver [7]. Received noise and interference can potentially degrade the performance of the CTL and corrupt the quality of these carrier phase measurements. The performance of a CTL can be evaluated in terms of its total phase jitter σ_φ, which is given as [2]:

$$\sigma_\varphi = \sqrt{\sigma_{\varphi_o}^2 + \sigma_{\delta_\varphi}^2} \tag{1}$$

This total phase jitter is composed of two significant components: the estimated output phase jitter σ_{φ_o} and the tracking error jitter σ_{δ_φ}.

A. Estimated Output Phase Jitter σ_{φ_o}

The estimated output phase jitter σ_{φ_o} reflects how much noise and interference in the incoming signal can be rejected during CTL operation, and can be given as [2]:

$$\sigma_{\varphi_o} = \sqrt{\frac{B_L}{C/(N_o + I)} \left(1 + \frac{1}{2TC/(N_o + I)}\right)} \tag{2}$$

where B_L denotes the tracking loop's bandwidth, $C/(N_o + I)$ denotes the CNIR and T denotes the integration duration. Equation (2) suggests that B_L needs to be minimised in order to reduce the effect of noise on the estimated output phase jitter σ_{φ_o}. However, reduction in B_L demands a consideration of the other major contributor to the total phase jitter: the tracking error jitter σ_{δ_φ}.

B. Tracking Error Jitter σ_{δ_φ}

The tracking error jitter σ_{δ_φ}, arising at the output of the phase discriminator, as indicated in Figure 1, can be expressed as [2]:

$$\sigma_{\delta_\varphi} = \sigma_{\delta_{\varphi c}} + \frac{\sigma_{\delta_{\varphi p}}}{3} \tag{3}$$

where $\sigma_{\delta_{\varphi p}}$ denotes the dynamic stress error, which for a 3rd order loop is given by [2]:

$$\sigma_{\delta_{\varphi p}} = \frac{2\pi(5.67)j_{max}}{\lambda B_L^3} \tag{4}$$

where j_{max} denotes the maximum value of jerk experienced by the receiver and λ denotes the carrier wavelength. A 3rd order loop is considered here, as it is the same as used in a Locata rover receiver. Also, $\sigma_{\delta_{\varphi c}}$ in (3) denotes the correlated phase errors and can be expressed as [2]:

$$\sigma_{\delta_{\varphi c}} = \sqrt{\sigma_{\delta_{\varphi TX}} + \sigma_{\delta_{\varphi RX}} + \sigma_{\delta_{\varphi v}}} \tag{5}$$

Here $\sigma_{\delta_{\varphi TX}}$, $\sigma_{\delta_{\varphi RX}}$ and $\sigma_{\delta_{\varphi v}}$ denote the errors due to transmitter clock, local oscillator and platform vibration respectively.

Vibration induced phase error $\sigma_{\delta_{\varphi_v}}$ is due to the external phase noise caused when the platform, on which the receiver is mounted, is subjected to mechanical vibration. $\sigma_{\delta_{\varphi_v}}$, for a third order CTL, can be given as [6]:

$$\sigma_{\delta_{\varphi_v}} = \sqrt{2\pi f_o^2 \int_0^\infty \frac{k_g^2(\omega)G_g(\omega)\omega^4}{\omega_L^6 + \omega^6}d\omega} \tag{6}$$

where f_o is the carrier frequency, k_g is the oscillator's g-sensitivity in parts-per-g, G_g is the single-sided vibration spectral density, ω is the vibration radian frequency and ω_L is a function of B_L and can be determined, considering the loop implementation [6].

As opposed to $\sigma_{\delta_{\varphi_v}}$ reflecting external phase noise, and $\sigma_{\delta_{\varphi_{TX}}}$ and $\sigma_{\delta_{\varphi_{RX}}}$ reflect the oscillator's natural phase noises at the transmitter and the receiver end respectively. Such phase noises resulting from oscillator instabilities can be described as [6]:

$$\sigma_{\delta_{\varphi_{osc}}} = \sqrt{2\pi f_o^2 \int_0^\infty \left[\frac{2\pi^2 h_{-2}}{\omega^4} + \frac{\pi h_{-1}}{\omega^3} + \frac{h_o}{2\omega^2}\right]\frac{\omega^6}{\omega_L^6 + \omega^6}d\omega} \tag{7}$$

where, h_{-2}, h_{-1} and h_o are the oscillator coefficients, which need to be derived experimentally.

Trends of these individual sources of error against different values of CTL bandwidth are depicted in Figure 2. It can be seen that errors due to dynamic stress, and external and natural phase noise errors, dominate at the low CTL bandwidths, and errors contributed by the received noise and interference dominate at higher values of CTL bandwidths. A low cost TCXO is used by both the Locata transmitter and receiver. Data for a generic TCXO and platform vibration, extracted from [2], has been used to plot the error profiles in Figure 2. Plots assume a value of 30dB-Hz and 0.25g for wide band noise and interference errors and dynamic stress errors respectively. Carrier frequency and wavelength are assumed to be those of the Locata S1 carrier. Figures 3 and 4 depict the total phase jitter plotted against BL and CNIR. The heavy lines at 15° in these two figures denote the theoretical upper limit of total phase jitter, which has been defined for an acceptable operation of a CTL [7]. This means that in order to avoid loss of lock, the loop's total phase jitter needs to be minimised. Figure 4 suggests that operation at low CNIR values, reduced by noise, interference and/or jamming, is possible if the total phase jitter at these values can be reduced. This can be achieved by reducing the effect of either of the two contributors: the estimated output phase jitter σ_{φ_o} or the tracking error jitter σ_{δ_φ}. Reduction in σ_{φ_o} is possible if the CTL operates at a lower B_L as noted in Section 2.1. Relationships presented in Section 2.2 and Figure 2 suggest that the jitter introduced by platform dynamics, receiver clock errors and mechanical vibration sets a lower limit on the extent to which this bandwidth B_L can be decreased. For loops without aiding, this lower limit varies from 10 - 18Hz depending on the application. If errors contributing to the total phase jitter can be estimated using external information, this can be reduced further [2], making the tracking loop more stable in low CNIR situations. For GPS, if this aid is obtained from external

means (e.g. an INS), errors due only to platform dynamics can be estimated and the loop bandwidth (B_L) can be reduced to 2Hz before the loop starts becoming unstable [2]. However, the INS-aided-GPS configuration introduces synchronisation issues and other implementation problems. However, if the aiding is obtained from another tracking loop, it can help to estimate errors due to receiver clock and vibrations, in addition to dynamics-induced errors [8]. This statement is supported by the relationships in Equations (4), (6) and (7). The dynamic stress errors and the oscillator's external and natural phase noise errors are all directly related to the carrier frequency. If these errors can be obtained from one CTL, the same can be estimated for the other CTL, operating in the same receiver and tracking signals from the same transmitter, using an appropriate relationship between the carrier frequencies of the signal tracked by the two CTLs. This motivates the proposal for a carrier loop aiding scheme for Locata that can facilitate operations at lower CNIR values without the use of external aids.

III. ADAPTIVE LOOP AIDING

In a Locata receiver, four carrier loops track two signals at each of the two frequencies. Figure 5 shows the carrier chart, where A1 and A2 denote the two antennas and S1 and S6 are the two carrier frequencies. It is proposed that two of these four loops be operated with a wider bandwidth of 15-25Hz and the other two loops with a narrower bandwidth. Both of the narrow band loops (NBL) will receive aiding from either of the wide band loops (WBL), depending upon their performance. An aiding loop's total phase jitter has been selected as the performance parameter here. As both the WBL will be tracking the same platform's dynamics and their carrier frequency ratio is close to unity, their total phase jitter will differ mainly due to their CNIR. If interference is received at one of the frequencies, as discussed before, affecting the total phase jitter of the WBL at that frequency, both NBL will switch to the other, interference-free, WBL for aiding. In this way, both NBL will receive interference-free aiding, unless interference corrupts both frequencies. In this situation, both NBL will still obtain aiding from the less affected WBL, making their estimates relatively less noisy. In a real world scenario, received noise and interference is likely to affect operation for loops tracking carriers at either or both of the frequencies. Using this scheme, the least affected of the two WBL will be adaptively selected to aid both NBL, where the WBL will handle dynamics and errors due to other sources and the NBL will reject interference. It can be observed from Figure 2 that at higher values of B_L, thermal noise and interference errors dominate. This scheme allows operation at lower B_L, where errors due to this noise and interference are less significant. This is achieved by removing the burden of tracking signal dynamics from the aided loops.

In order to explore how the loop aiding works mathematically, consider the signal reaching the tracking loop

represented by:

$$y_i(t) = A\sin(2\pi(f_{rel} + f_{osc} + f_{vic} + f_{oth})t + \theta_i) \tag{8}$$

where A = received signal amplitude

f_{rel} = Doppler frequency due to platform dynamics

f_{osc} = oscillator-induced frequency errors

f_{vib} = vibration-induced frequency errors

f_{oth} = frequency errors due to troposphere, noise and interference and other unmodelled errors

θ_i = carrier phase at phase detector

Also, the incoming signal's estimate generated by the aiding and the aided loop can be given as:

$$\hat{y}_i(t) = B\sin(2\pi(\hat{f}_{rel} + \hat{f}_{osc} + \hat{f}_{vib} + \hat{f}_{oth})t + \varphi) \tag{9}$$

where $\hat{f}_{rel}$, $\hat{f}_{osc}$, $\hat{f}_{vib}$ and $\hat{f}_{oth}$ denote the estimated error quantities. Now the multiplier uses the received signal and the locally generated estimate to generate the error signal given by:

$$y\hat{y}_i(t) = C\sin(2\pi(f_{est} + \acute{f}_{oth})t + \alpha) \tag{10}$$

Two quantities f_{est} and $\acute{f}_{oth}$ are introduced here which denote the estimation errors (difference between actual frequency errors at NBL and their estimates generated by WBL) and noise, interference and other unmodelled error differences. The frequency sum term generated by the multiplier will be removed by the loop filter and is therefore not mentioned further. The in-phase and quadrature components can be written as:

$$y\hat{y}_I(t) = C\sin(2\pi(f_{est} + \acute{f}_{oth})t + \alpha)$$
$$y\hat{y}_Q(t) = C\cos(2\pi(f_{est} + \acute{f}_{oth})t + \alpha) \tag{11}$$

Effectively the NBL now has to track errors $f_{est} + \acute{f}_{oth}$ which are (relatively) less than the actual errors. As a result a very low bandwidth can be used to track these errors.

In order to determine the proportion of contributions made by the aiding and aided loop to constitute the aided loop's estimated output phase φ_o, a conventional approach can be employed. First consider the situation for an unaided loop, as shown in Figure 6. Here $\theta_i(z)$ denotes the phase of the input signal and $\theta_o(z)$ $(= Z\{\varphi_o\})$ denotes the phase of the VCO output. The phase detector generates a voltage signal $(V_d(z))$ proportional to the difference between the received and the estimated phases:

$$V_d(z) = K_d(\theta_i(z) - \theta_o(z)) \tag{12}$$

where K_d is the gain of the phase detector. This voltage signal is filtered using the loop filter $F(z)$ for suppressing noise and higher frequency components and the resulting voltage signal $V_c(z)(= F(z)V_d(z))$ is used to control the

VCO. The VCO here amplifies the received signal using the gain factor K_o and integrates the resulting signal to generate the estimated output phase $\theta_o(z)$.

This conventional loop can be modified to obtain the desired expression for the aided loop's estimated output phase. The loop aiding architecture is illustrated in Figure 7. From this figure, estimated output phase $\theta_o(z)$ for the aided loop can be given as:

$$\theta_o(z) = N(z)V_{comp}(z) \tag{13}$$

where $V_comp(z)$ is the composite voltage given by:

$$V_{comp}(z) = V_a(z) + V_c(z) \tag{14}$$

where,

$$V_a(z) = SV_c'(z) \tag{15}$$

with

$$S = \frac{f_{aided}}{f_{aiding}} \tag{16}$$

Here $V_c'(z)$ is the voltage signal proportional to the aiding loop's signal dynamics and $V_c(z)$ is the voltage signal proportional to the aided loop's estimate of residual signal dynamics that it tracks. Now, Equation (13) can be expanded using Equation (14) to give:

$$\theta_o(z) = N(z)(V_a(z) + F(z)V_d(z)) \tag{17}$$

Also, by using Equation (12), Equation (17) can be rewritten as:

$$\theta_o(z) = N(z)V_a(z) + N(z)F(z)K_d(\theta_i(z) - \theta_o(z))$$

$$\theta_o(z) = N(z)V_a(z) + K_d N(z)F(z)\theta_i(z) - K_d N(z)F(z)\theta_o(z)$$

$$\theta_o(z) = \frac{N(z)V_a(z) + K_d N(z)F(z)\theta_i(z)}{1 + K_d N(z)F(z)}$$

$$\theta_o(z) = \frac{N(z)}{1 + K_d N(z)F(z)}V_a(z) + \frac{N(z)F(z)}{1 + K_d N(z)F(z)} \tag{18}$$

where $V_i(z)(= K_d\theta_i(z))$ is the voltage signal proportional to the phase of the signal received at the input of the aided loop. Equation (18) represents the proportion in which aiding and aided loops' contributions are combined to constitute the aided loop's estimated output phase. In the simulations that follow a software based receiver is used, where the VCO is replaced by an NCO for which the transfer function is:

$$N(z) = \frac{K_o z^{-1}}{1 - z^{-1}}$$

where K_o denotes the NCO gain.

IV. PREDICTION OF LOWER BOUND

It must be emphasised that in this scheme, aiding is obtained from another loop, instead of some external device such as an INS. For this reason, although the errors due to platform dynamics, vibration and local oscillator (receiver clock) are reduced, additional phase errors due to noise and interference are induced from the aiding loop. This introduces a composite noise error in the final signal generated by the aided loop's NCO. This composite error can be expressed as:

$$\sigma^2_{\varphi_o,comp} = \sigma^2_{\varphi_o(aiding)} + \sigma^2_{\varphi_o(aided)} + 2\sigma^2_{\varphi_o(aiding,aided)} \tag{19}$$

where $\sigma^2_{\varphi_o(aiding,aided)}$ denotes the aiding and aided loops' noise and interference error covariance. Equation (19) states that the total phase jitter of the aided loop will consist of these composite errors in addition to estimation and other unmodelled errors. Therefore Equation (19) suggests a lower bound on the total phase jitter of the aided loops, as these will be present even if the signal dynamics estimates are very close to the actual values.

Also, Equation (19) suggests a relationship between the aided loop's total phase jitter and the quality of the signal tracked by the aiding loop. For the aided loop to perform better would require a relatively interference-free and less noisy estimate from the aiding loop. Where the aiding loop's measurements are corrupted by received interference, the aided loop's performance will also be degraded. A loss of lock can also occur for the aided loop in this situation depending upon the quality of the aiding information. Such a situation can be predicted using Equations (2) and (19) if the individual CNIR are known.

V. SCHEME IMPLEMENTATION

In order to analyse the proposed method, Locata signals were simulated according to the available specifications [9], and were processed using a modified software receiver [15]. Different scenarios were simulated, where interference on either or both of the frequencies was considered. The same vehicle dynamics profile, as shown in Figure 8, was considered for all tests.

A. Unaided Loop Performance

First consider the tracking performance of an unaided loop plotted in Figures 9 and 10 in terms of phase jitter plotted against loop bandwidth (B_L) and CNIR. It can be readily noticed here that the phase jitter is significantly dependent on B_L for all values of CNIR. At lower values of B_L the phase jitter curves for different values of CNIR start to converge. This convergence occurs due to the fact that at this point, noise- and interference-induced errors become less dominant compared to signal dynamics-induced errors which are common for all the curves. This convergence point is jointly determined by the signal dynamics and CNIR. Signal dynamics and the thermal

noise plus received interference set the upper and lower bounds on the BL. This results in a trade-off for an optimal value of B_L to minimise this phase jitter. This can be understood by noting the error trends in Figure 2. The errors due to signal dynamics tend to increase at lower B_L, while at higher B_L wide band noise+interference-induced errors become dominant. These two factors jointly set a minimum achievable phase jitter value. From Figure 9 it can also be observed that for a B_L of 8Hz the loop operated very close to 15° threshold. It was found that the carrier loop was not able to maintain lock at B_L 7Hz or less for the vehicle dynamics defined by Figure 8.

B. Aided Loop Performance

It was discussed above that in order to reduce the phase jitter, the effect of at least one of the abovementioned factors needs to be reduced. One possible way of achieving this, as discussed above, is by obtaining external or internal estimates of signal dynamics. In the proposed method the signal dynamics estimates are obtained from another carrier loop with a wider bandwidth operating at a frequency which may or may not be the same. This aiding from either a co-frequency or cross-frequency loop removes the burden of signal dynamics estimation from the aided loop, thus allowing it to operate at a lower B_L. Operation at lower bandwidths facilitates noise rejection, making it possible to track signals with reduced CNIR values.

Figures 11 and 12 depict the situation after implementation of the proposed method and are directly comparable to Figures 9 and 10 (the same scales are used, explaining the relative sparseness of Figure 9). Here the aiding WBL were operated with a B_L of 25Hz. Wideband white noise+interference was alternatively introduced into one of the two signals tracked by the WBL, while the other signal was kept at a fixed CNIR of 53dB-Hz. Both the NBL observed the jitter estimates from both the WBL and used the less noisy ones, after appropriate scaling according to frequency ratios (S). It was observed that the NBL at the frequency suffering interference was able to maintain lock at bandwidths down to 0.5Hz. Below this bandwidth the loop was not able to maintain lock at any of the tested CNIR values. This threshold of 0.5Hz for loss of lock was the same for all tested CNIR values because all curves converged at this point. The shifting of the convergence point to a lower B_L value can be explained as follows. In the unaided case, errors due to signal dynamics dominated at 8Hz as compared to noise- and interference-induced errors. However, in the case of aided loops, errors due to signal dynamics were reduced by removing the burden of tracking full signal dynamics from the aided loop. Signal dynamics thus did not become dominant again until the noise- and interference-induced errors became much weaker at 0.5Hz.

Looking at the situation in a different way, Figure 12 shows the phase jitter values plotted against CNIR for the aided loop operating at different bandwidths. It was observed that the aided loop was able to maintain lower jitter at higher CNIR, while operating with a wider B_L. However, at lower values of CNIR, the loop with these wider

bandwidths lost lock before the one with a narrower bandwidth. This was due to the fact that at higher bandwidths jitter due to noise and interference dominates, which keeps the loop from maintaining lock at low CNIR values. In an unaided situation, a loop fails to remain in lock at narrower B_L due to increased phase jitter induced by signal dynamics. Aiding here lessens its influence by providing a signal dynamics estimate allowing operate with narrower B_L and permitting it to remain locked at lower CNIR values. The fact that the effects of signal dynamics are reduced is also confirmed by the movement of the minimum jitter point from a higher B_L to a lower B_L for signals with reduced CNIR.

Figure 10 shows that in an unaided situation, with a loop bandwidth of 10Hz, the 15° theoretical limit is exceeded when the signal level dropped below 27dB-Hz. However, it can be seen from Figure 12 that the phase jitter did not exceed this limit until the signal level dropped below 21.5dB-Hz, while operating with a loop bandwidth of 1Hz. This shows that a margin of 5.5dB-Hz was achieved, under simulation conditions, against received wide band noise+interference, as the loop was able to operate with a narrower bandwidth and therefore rejected more noise.

To this point the aiding loop has been assumed to be tracking a signal at 53dB-Hz. In a real-world scenario this may not be the case. It is highly likely that CNIR would degrade and/or fluctuate due to various factors, particularly due to received interference. It may be the case that the interference is received at both of the frequencies. In this case CNIR will be reduced for the signals tracked by both the aiding loops. Therefore, in order to explore the proposed method further the aiding loop was made to track signals with different CNIR values. Interference was assumed to be present at both frequencies. This made the CNIR for both the aiding signals degrade from an optimistic value of 53dB-Hz. Performance of aided loops, in this situation, in terms of phase jitter is depicted in Figures 13 and 14. For this test, the aided and the aiding loop were operated with 2Hz and 25Hz bandwidths respectively. CNIR of the signal tracked by aiding loop was varied in the range 53 - 33dB-Hz, while for the aided loop it was kept fixed at 30dB-Hz. It can be observed from Figure 13 that the aided loop lost lock at a bandwidth similar to the previous aided case. This was due to the fact that as the aiding loop's bandwidth remained fixed at a high value, the quality of signal dynamics estimates was less affected. This kept the aided loop's jitter at similar values at lower bandwidth, while it degraded for higher bandwidths due to the aiding signal's degraded CNIR. Another interesting point to note here is that, in this case, the minimum achievable jitter (MAJ) value increased as the aiding signal's CNIR decreased. Here MAJ can be defined as the minimum achievable jitter while tracking a signal with a given CNIR, which will be the lowest point in each curve in this figure. The observed increase in the MAJ is in accordance with Equation (19). As expected, a relationship between the quality of the signal tracked by aiding loop and the performance achievable by the aided loop can be easily noted here. Figure 14 illustrates the same fact, where reflection of the aiding loop's signal quality degradation can be noted in the aided loop's achieved

jitter at various CNIR. The observations discussed above, and the fact the aided loop's performance is dictated by the aiding signal quality, suggest that a lower limit on the aiding loops' performance needs to be set in order to gain advantage from the proposed method.

To further evaluate the proposed method's performance, the aiding loop's bandwidth was varied while keeping the aiding signal's CNIR constant. Again the aiding loop was operated at 53dB-Hz, with loop bandwidth varying in the range 10 - 25Hz. Figures 15 and 16 show the aided loop's performance for such a situation where phase jitter is plotted against the aided loop's B_L and CNIR. It can be noted that as the aiding loop's bandwidth was reduced, the quality of its signal dynamics estimates degraded. This situation can particularly be noticed while the aided loop operated at lower loop bandwidths. From Figure 15 it can be observed that at a higher aided loop bandwidth ($B_{L(aided)}$), jitter remained unaffected while the aiding loop bandwidth ($B_{L(aiding)}$) was varied. This was due to the fact that with high loop bandwidth, the aided loop was able to handle the signal dynamics itself and did not rely as much on the dynamics estimates from the aiding loop. Conversely, for low values of $B_{L(aided)}$, phase jitter increased as the $B_{L(aiding)}$ was reduced, as the aided loop relied on the quality of signal dynamics estimates from the aiding loop, for improved performance. This reduction in $B_{L(aiding)}$ also degraded the minimum achievable phase jitter.

VI. ADAPTIVE KALMAN FILTER BASED LOOP AIDING

Results presented above show that an loop aiding can potentially reduce phase jitter, offering a margin of 5.5dB-Hz against received noise and interference. However, some residual noise still leaks through the aided loop's narrow filter. This residual noise is contributed not only by the received noise entering the aided loop but also by that from the aiding loop, as discussed in Section 4 and observed from results presented in Section 5. This suggests that there exists room for improvement in terms of noise rejection in the aided loop's measurements, if the aiding loop's estimates can be made less noisy. The authors propose the use of a Kalman filter for this purpose. For a standalone CTL, a Kalman filter (KF) has also been extensively researched to provide carrier phase measurements with reduced noise [10], [11], [12]. Typically a KF either reduces noise in a loop filter's estimates or replaces the loop filter altogether to generate less noisy estimates. In order to further improve the method described in Section 3, loop aiding was performed by employing a KF-based architecture.

Kalman filtering is a common approach for estimating the state of a noisy process. The KF achieves this objective by employing an iterative-in-time prediction-correction model represented by the following model equations:

1) Prediction Model:

$$\hat{x}_k^- = A\hat{x}_{k-1} + Bu_k$$

$$P_k^- = AP_{k-1}A^T + Q$$

(20)

2) Correction Model:

$$K_k = P_k^- H^T (HP_k^- H^T + R)^{-1}$$

$$\hat{x}_k = \hat{x}_k^- + K_k(z_k - H\hat{x}_k^-)$$

(21)

$$P_k = (I - K_k H)P_k^-$$

where x denotes the state vector to be estimated, ˆ denotes the estimated element, superscript-minus ($^-$) indicates

a priori nature of the element, A is the state transition matrix, B is the input transmission matrix, P is the error

covariance, K is the Kalman gain, z is the measurement vector, H is the measurement matrix and Q and R denote

the covariances of the process noise w and measurement noise v respectively. Here the modelled noise statistics

Q and R tune the Kalman filter for smooth tracking. Accuracy of these noise models, which potentially contribute

to the performance of the KF, depends on *a priori* knowledge of system application and process dynamics, which

is difficult to obtain in practice [13]. Therefore approximate models can serve as a possible solution in such

situations. However, during sudden manoeuvres, like rapid changes in trajectory (for instance, sharp turns), such

approximate models cannot replicate dynamics accurately leading to divergence of the KF, causing "overshoots".

This happens due to the fact that the KF tries to maintain the previous trajectory and takes time to adjust to sudden

changes. Adjusting these approximations can either "tighten" the Kalman filter, resulting in higher noise rejection

and generating overshoots, or vice versa. This is a classic trade-off between dealing with dynamics and rejecting

noise. In such cases an adaptive KF algorithm provides a better solution at the expense of increased complexity. An

adaptive Kalman filter (AKF) dynamically adjusts the modelled noise statistics by estimating Q and/or R "on the

fly". One possible approach to determine Q and R can be given as follows: Defining the measurement innovation

v_k, as the difference between the actual measurement and its predicted value, it can be given as:

$$v_k = z_k - H\hat{x}_k^-$$

(22)

Using Equation (22), the innovation covariance matrix is:

$$C_k = E(v_k v_k^T) = HP_k^- H^T + R_k$$

(23)

This innovation covariance matrix can be employed to obtain Q and/or R using the following relationships [13]:

$$R_k = C_k - HP_k^- H^T$$

$$Q_k = K_k C_k K_k^T$$

(24)

A. Proposed Scheme Augmentation

To reduce the aided loop's residual noise in two stages, a cascade of Adaptive Kalman filters is used to augment the loop aiding architecture. This cascade combines carrier phase measurements from all four carrier loops tracking signals from the same LocataLite and generates the less noisy state estimates: carrier tracking error (δ_φ) and carrier NCO updates (φ') for the aiding and the aided loops by minimising the error covariance of these estimates. The first filter of the cascade operates on the noisy carrier error measurements from the wide band aiding loops and estimates less noisy carrier NCO updates for these loops. The less noisy of the two updates is selected and used to produce the signal dynamics estimates for the aided loops using the relationship S between the aiding and the aided signal's carrier frequencies. At this stage, the first KF not only reduces noise in the WBL's NCO updates, but also makes the aiding signal dynamics estimates less noisy. The aided loops' carrier tracking error measurements and the signal dynamics estimates originating from the aiding loop serve as input for the second filter that estimates carrier NCO updates for the aided loops. As both of these two inputs are corrupted by the residual noise as discussed in the previous section, the second KF operates to reduce this residual noise and to generate smoothed updates for the aided loops. A modified loop structure is shown in Figure 17. The state vectors x, state transition matrices A and input transmission matrices B for the first and second KFs of the cascade are proposed as follows.

1) 1st Kalman Filter

$$x_1 = \begin{bmatrix} \delta_{\varphi_{1,aiding}} \\ \varphi'_{1,aiding} \\ \delta_{\varphi_{2,aiding}} \\ \varphi'_{2,aiding} \end{bmatrix}$$

$$A_1 = \begin{bmatrix} 1 & 0 & 0 & 0 \\ -\dfrac{\tau_2}{\tau_1}\Bigg|_{1,aiding} & 1 & 0 & 0 \\ 0 & 0 & 1 & 0 \\ 0 & 0 & -\dfrac{\tau_2}{\tau_1}\Bigg|_{2,aiding} & 1 \end{bmatrix} \tag{25}$$

$$B_1 = \begin{bmatrix} 0 & 0 \\ -\dfrac{\tau_2 + T}{\tau_1}\bigg|_{1,aiding} & 0 \\ 0 & 0 \\ -\dfrac{\tau_2 + T}{\tau_1}\bigg|_{2,aiding} & 0 \end{bmatrix}$$

2) 2nd Kalman Filter

$$x_1 = \begin{bmatrix} \delta_{\varphi_{3,aiding}} \\ \varphi'_{3,aiding} \\ \delta_{\varphi_{4,aiding}} \\ \varphi'_{4,aiding} \end{bmatrix}$$

$$A_1 = \begin{bmatrix} 1 & 0 & 0 & 0 \\ -\dfrac{\tau_2}{\tau_1}\bigg|_{3,aided} & 1 & 0 & 0 \\ 0 & 0 & 1 & 0 \\ 0 & 0 & -\dfrac{\tau_2}{\tau_1}\bigg|_{4,aided} & 1 \end{bmatrix}$$

$$B_1 = \begin{bmatrix} 0 & 0 & 0 & 0 \\ -\dfrac{\tau_2 + T}{\tau_1}\bigg|_{1,aiding} & \beta_1 & 0 & 0 \\ 0 & 0 & 0 & 0 \\ 0 & 0 & -\dfrac{\tau_2 + T}{\tau_1}\bigg|_{2,aiding} & \beta_1 \end{bmatrix}$$

(26)

where τ_1 and τ_2 denote the carrier loop coefficients, T denotes the pre-detection integration duration and β denotes the carrier frequency dependent scaling factor. The process noise models for the first and second KFs can be given as:

$$w_1 = [\sigma^2_{\delta_{\varphi_1}} \quad \sigma^2_{\varphi'_1} \quad \sigma^2_{\delta_{\varphi_2}} \quad \sigma^2_{\varphi'_2}]$$
$$w_1 = [\sigma^2_{\delta_{\varphi_3}} \quad \sigma^2_{\varphi'_{3,m}} \quad \sigma^2_{\delta_{\varphi_4}} \quad \sigma^2_{\varphi'_{4,m}}]$$

(27)

where $\sigma^2_{\delta_{\varphi_n}}$ and $\sigma^2_{\varphi'_n}$ define carrier tracking error and carrier NCO update estimation process noise respectively, and m denote the aiding loop. By definition, the process and the measurement noise statistics are:

$$P(w) \sim N(0, Q)$$

$$Q = E[w_k w_k^T]$$

$$P(v) \sim N(0, R)$$

$$Q = E[v_k v_k^T]$$

(28)

B. Performance Evaluation and Comparison

This sub-section analyses the CTL performance for the above mentioned scenarios, discussed in Section 5.2, using an AKF-based loop aiding (LA-AKF) architecture. First consider the scenario where the aiding loops operate with a bandwidth of 25Hz while tracking a signal with a CNIR of 53dB-Hz. The performance of the aided loop is evaluated for bandwidths up to 40Hz while tracking signals with different CNIR. Figures 18 and 19 show the results where the loop performance is plotted in terms of phase jitter against tracking loop bandwidth and tracked signal's CNIR. It was observed that the LA-AKF was unable to operate at B_L less than 0.5 Hz, as was the case with the aided loop without Kalman filter (LA-NKF). However the main point of concern will be the improvement in terms of minimum achievable jitter (MAJ) while tracking signals with low CNIR. By comparing Figure 18 with Figure 11 it can be noted that, for tracked signals with CNIR less than 43dB-Hz, the LA-AKF further reduced the MAJ compared to the LA-NKF. Considering the worst quality signal, with a CNIR of 23dB-Hz, the LA-AKF was able to track it with an MAJ value of 9.5^o as compared to the LA-NKF which tracked the same signal with an MAJ value of 12.5^o; a 3° margin. Also, the LA-AKF was able to maintain a lower phase jitter value at higher $B_{L(aided)}$ for signals with degraded CNIR. Analysing the improvement from another perspective, a comparison of Figures 19 and 12 illustrates that while the LA-NKF tracked signals with a minimum CNIR value of 21.5dB-Hz, the LA-AKF was able to track signals down to a CNIR of 19dB-Hz before it crossed the 15° phase jitter threshold, offering a margin of 2.5dB-Hz over the LA-NKF under simulation conditions. Also at moderate CNIR values, the LA-AKF performed better than the LA-NKF, as can be noted by comparing Figures 19 and 12. These improvements were achieved mainly due to the fact that in case of the LA-AKF, not only the aided loops rejected noise by operating at a smaller B_L, but also the aiding loop estimates were made less noisy using the AKF, before these were injected into the aided loop. The second stage KF in the KF cascade also contributed to this improvement by statistically minimising the error covariance during the aiding process. There is a significant point to note here. In the case of the LA-NKF, jitter due to received noise and interference can be reduced further by decreasing the aided loop's bandwidth. However, this is at the cost of making the loop more vulnerable to signal dynamics. The LA-AKF offers

improvement in rejecting incoming noise and interference without making the loop vulnerable to signal dynamics and loss of lock as the LA-AKF does not require further reductions in loop bandwidths.

Considering a real-world scenario, the aiding signals' CNIR was degraded from an ideal value of 53dB-Hz and was tracked with a CTL with 25Hz bandwidth. Figures 20 and 21 illustrate these results, where the CTL's performance is plotted again in terms of its phase jitter against B_L and CNIR. Some important observations can be made here by comparing these figures with the LA-NKF results presented earlier in Figures 13 and 14. Comparing the LA-AKF performance in Figure 20 against that of the LA-NKF in Figure 13, it can be noted that the LA-AKF resisted performance degradation better in terms of MAJ as the aiding signal's CNIR was reduced. This was mainly due to the fact that the added noise in the aiding signal was rejected by the KF cascade, which was not the case for the LA-NKF. For the set of results shown in this figure the aided signal was kept at 30dB-Hz CNIR. Similar observations can be made from Figure 21, where phase jitter is plotted against CNIR, while the aided loop operates with a bandwidth of 2Hz. Due to the fact that a corrupted aiding signal can degraded aided loop's performance, it was identified in Section 5.2 that a lower limit needed to be set on the aiding signal quality so that the aided loop's performance remains within acceptable limits. The fact that the LA-AKF performance, as compared to that of the LA-NKF, degrades less while the aiding signal quality gets corrupted by same amount of noise and interference, suggests that this limit can be further lowered and a lower quality signal can be used for aiding.

To further explore the improvement offered by the proposed augmentation, $B_{L(aiding)}$ was varied in the range of 10-25Hz while tracking the aiding signal at 53dB-Hz. Figures 22 and 23 depict this situation. Here, again an improvement as compared to LA-NKF can be noticed, as LA-NKF better rejected the noise. By comparing Figures 22 and 23 with Figures 15 and 16, it can be noticed that jitter was reduced for lower values of aided signal's CNIR. This contribution was mainly made by the second stage KF which rejected noise in the aided signal's estimates.This comparison also shows that although the performance of LA-AKF degraded as the $B_{L(aiding)}$ was reduced, this degradation was lesser than in case of LA-NKF.

For all the simulations in this paper it was assumed that all CNIR variations were mainly due to the received noise and interference and were not affected by Locata receiver movements away or towards the LocataLites. Also, although tracking of low CNIR signals can be facilitated by the use of longer integration durations or, alternatively, signal dynamics can be handled by faster loop updates, both of these parameters were kept constant during the subsequent analyses. This was done in order to produce standardised results, independent of these two parameters. It is important to note that the results presented here are valid for the given set of dynamics and white noise and interference, and may vary depending upon the type of dynamics and interference involved. However, results in such cases can still be predicted using the mathematical relationships presented in the paper if the nature of dynamics

and type received interference is known.

VII. CONCLUSION

An adaptive inter-loop aiding scheme is proposed and analysed in this paper. The proposed scheme's performance is evaluated with and without the use of an Adaptive Kalman filter. This scheme employs the concept of loop aiding without requiring any external estimates. It is established that the inter-loop aiding improves the CTL performance by reducing its phase jitter and allowing tracking of signals with CNIR values reduced by wide band noise and interference. Performance improvement is shown to be achieved when either or both of the carrier frequencies are affected by received noise and interference. It is shown that, under simulation conditions, a margin of 5.5dB-Hz can be achieved while operating at 0.5Hz loop bandwidth without using Adaptive Kalman filtering. It is identified that an adaptive Kalman filter-based loop aiding approach improves this margin by 2.5dB-Hz. It is also established that, in the absence of the Kalman filter, the quality of the aiding signal and the aiding loop's bandwidth will potentially dictate the quality of aiding, and eventually the aided loop's performance. Considering this fact it is shown that a lower bound is predictable for the aided loop's performance. It is also shown that Adaptive Kalman filter-based loop aiding resists the degradation in aided loop's performance as the quality of the aiding signal degrades. It is also identified that in the case of the Adaptive Kalman filter-based aiding scheme improvements are obtained without making loops vulnerable to loss of lock, as the Adaptive Kalman filtering does not require further reduction in loop bandwidths.

REFERENCES

[1] F. A. Khan, A. G. Dempster, C. Rizos, "Locata-based Positioning in the Presence of WiFi Interference: Test Results," *21st Int. Tech. Meeting of the Satellite Division of the U.S. Inst. of Navigation*, Savannah, Georgia, September 2008, 2645-2649.

[2] D. G. Egziabher, A. Razavi, P. Enge, J. Gautier, D. Akos, S. Pullen, B. S. Pervan, "Doppler Aided Tracking Loops for SRGPS Integrity Monitoring," *16th Int. Tech. Meeting of the Satellite Division of the U.S. Inst. of Navigation*, Portland, Oregon, September 2003, 2562-2571.

[3] D. Megahed, C. O'Driscoll, G. Lachapelle, "Combined L1/L5 Kalman Filter-Based Tracking for Weak Signal Environments," *European Navigation Conference*, Naples, Italy, 3-6 May 2009.

[4] M. Ripley, J. Cooper, P. Daly, P. Silvestrin, "A Dual-Frequency GNSS Sensor for Space Applications," *International Journal of Satellite Communications*, 16(6), 1998, 273-282.

[5] O. Julien, "Carrier-Phase Tracking of Future Data/Pilot Signals," *18th Int. Tech. Meeting of the Satellite Division of the U.S. Institute of Navigation*, Long Beach, California, 13-16 September 2005, 113-124.

[6] M. Irsigler, B. Eissfeller, "PLL Tracking Performance in the Presence of Oscillator Phase Noise," *GPS Solutions*, 5(4), 2002, 45-57.

[7] E. D. Kaplan, C. J. Hegarty, "GPS: Principles and Applications," 2nd Edition, Artech House Publication, 2006.

[8] R. D. Fontana, W. Cheung, T. A. Stansell, "The New L2 Civil Signal," *14th Int. Tech. Meeting of the Satellite Division of the U.S. Inst. of Navigation*, Salt Lake City, Utah, 11-14 September 2001, 617-631.

[9] J. Barnes, C. Rizos, M. Kanli, A. Pahwa, D. Small, G. Voigt, N. Gambale, J. Lamance, "High Accuracy Positioning Using Locata's Next Generation Technology," *18th Int. Tech. Meeting of the Satellite Division of the U.S. Institute of Navigation*, Long Beach, California, 13-16 September 2005, 2049-2056.

[10] M. L. Psiaki, "Smoother-Based GPS Signal Tracking in a Software Receiver," *14th Int. Tech. Meeting of the Satellite Division of the U.S. Inst. of Navigation*, Salt Lake City, Utah, 11-14 September 2001, 2900-2913.

[11] M. L. Psiaki, H. Jung, "Extended Kalman Filter Methods for Tracking Weak GPS Signals," *15th Int. Tech. Meeting of the Satellite Division of the U.S. Inst. of Navigation*, Portland, Oregan, 24-27 September 2002, 2539-2553.

[12] K. H. Kim, G. I. Jee, J. H. Song "Carrier Tracking Loop using the Adaptive Two-Stage Kalman Filter for High Dynamic Situations," *International Journal of Control, Automation, and Systems*, 6(6), 2008, 948-953.

[13] A. H. Mohamed, K. P. Schwarz, "Adaptive Kalman Filtering for INS/GPS," Journal of Geodesy 73, 1999, 193 - 203.

[14] F. A. Khan, C. Rizos, A. G. Dempster, "Adaptive Loop Aiding for Performance Improvement in Weak Signal Environment", European Navigation Conference, Naples, Italy, 3-6 May.

[15] SoftGPS Project (2006) http://gps.aau.dk/softgps.

Faisal Ahmed Khan is currently a Ph.D. student at University of New South Wales. His main area of research is interference effects and analysis in positioning environment. He holds a M. Phil Degree from University of New South Wales, Australia and B.E. (Electronics) degree from NED UET, Pakistan. He has also gained hands-on experience in the field of Satellite Communications at Institute of Space Technology (IST), Pakistan and Pakistan Space and Upper Atmosphere Research Commission.

Andrew Dempster is Director of Research in the School of Surveying and Spatial Information Systems at the University of New South Wales (UNSW). He led the team that developed Australia's first GPS receiver in the late 80s and has been involved with satellite navigation ever since. His current research interests are GNSS receiver design, GNSS signal processing, and new location technologies.

Chris Rizos is currently Professor and Head of the School of Surveying and Spatial Information Systems, UNSW. Chris has been researching the technology and high precision applications of GPS since 1985, and has published over 400 journal and conference papers. He is a Fellow of the Australian Institute of Navigation and a Fellow of the International Association of Geodesy (IAG). He is currently the Vice President of the IAG and a member of the Executive of the International GNSS Service.
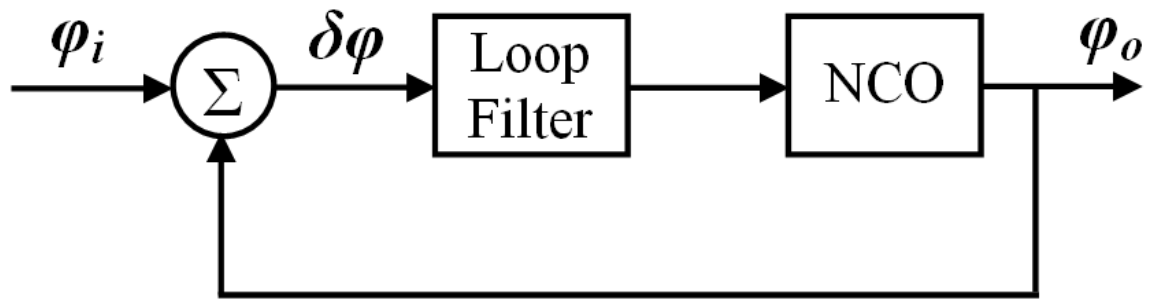
Fig. 1.   Generic Un-aided Carrier Tracking Loop
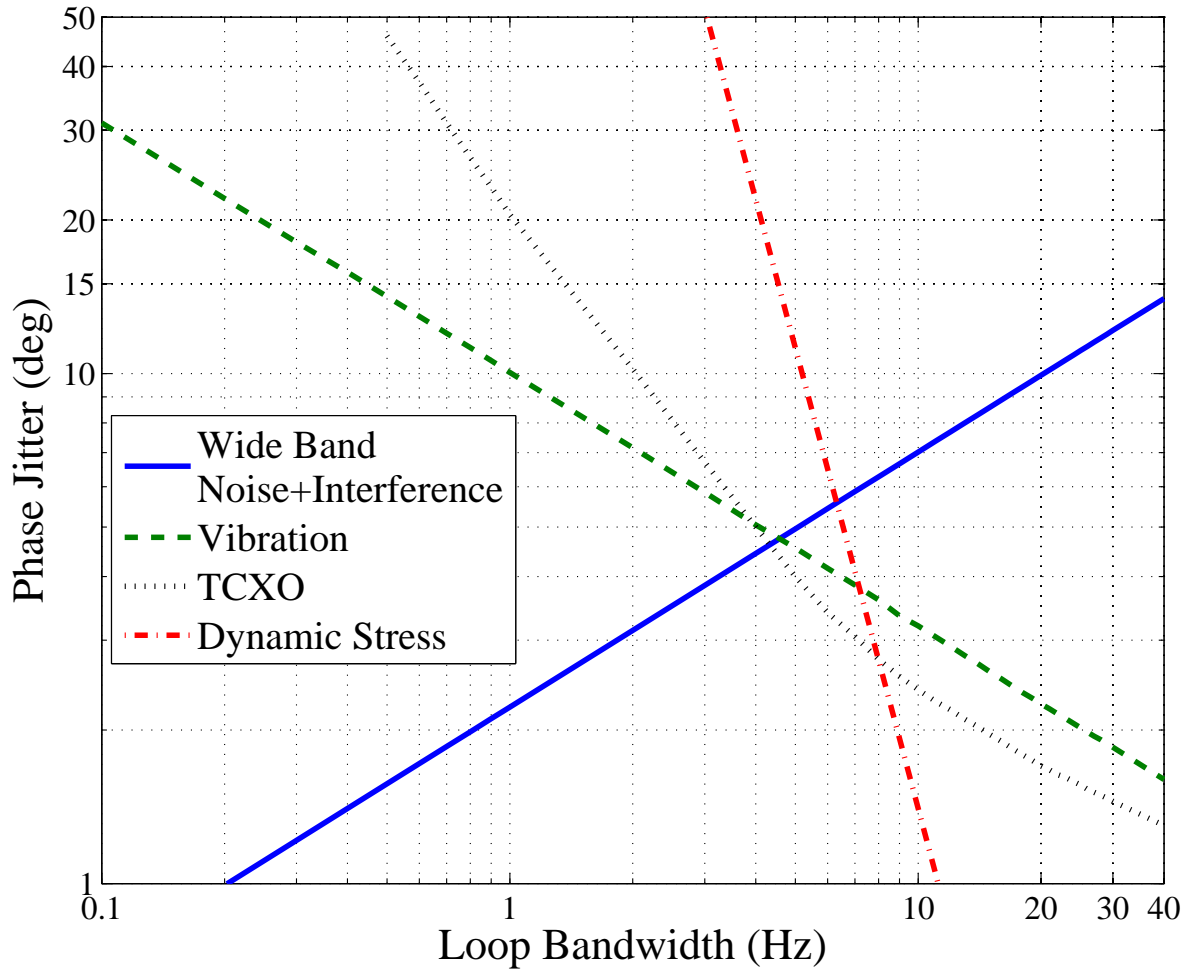
Fig. 2. Individual Sources of Error Contributing to Total Phase Jitter
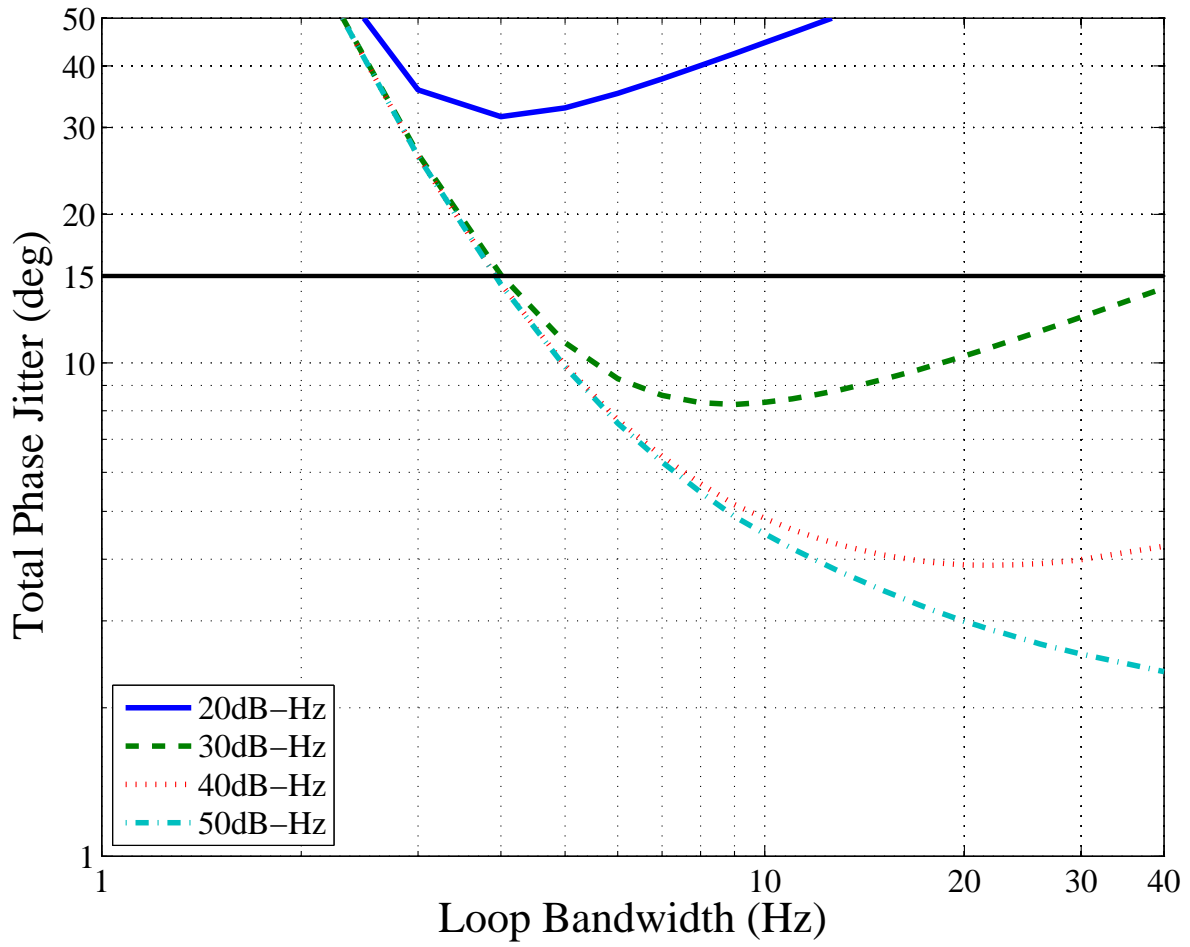
Fig. 3. Theoretical Total Phase Jitter against Loop Bandwidth for Different CNIR (Without Loop Aiding).
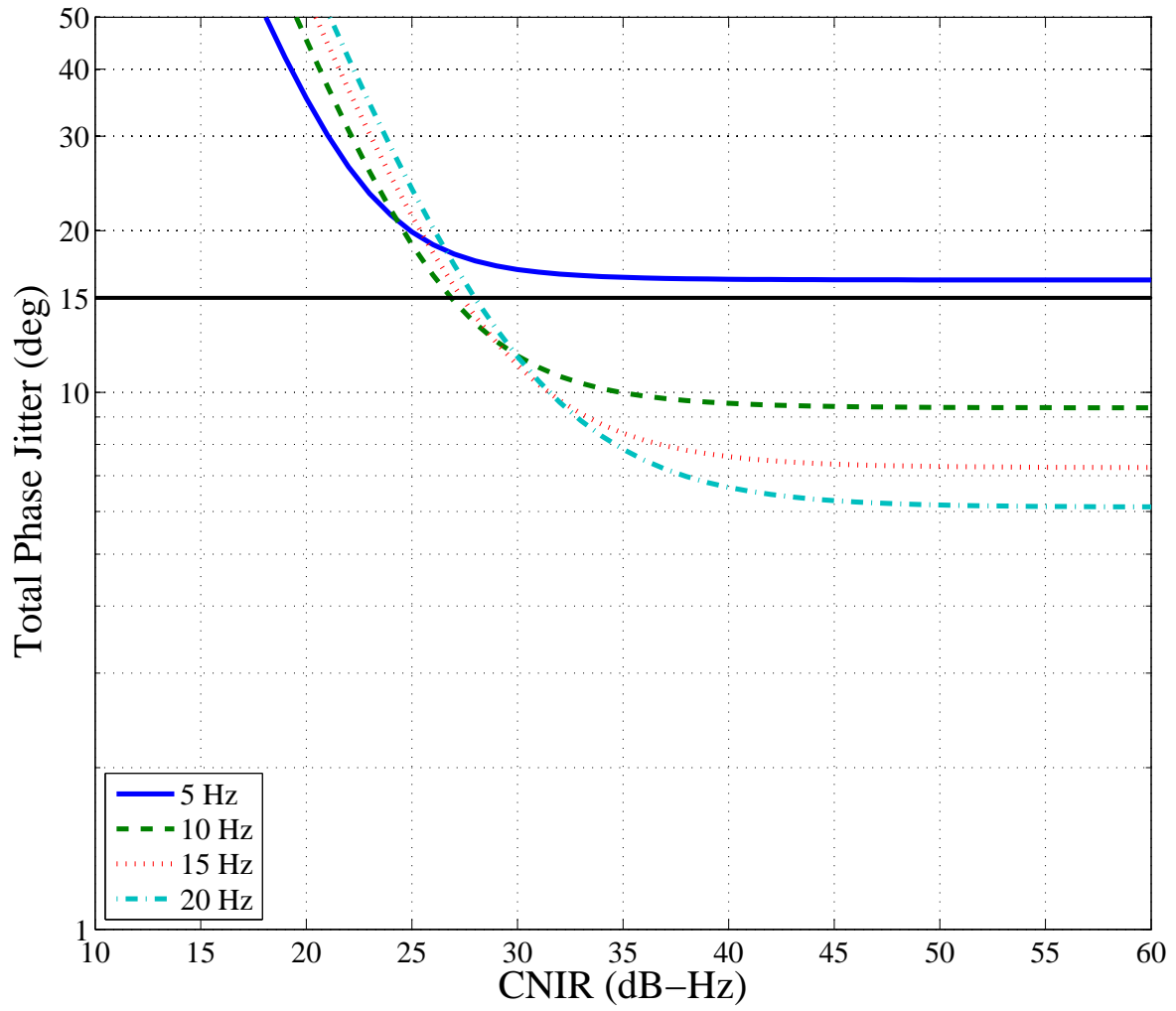
Fig. 4. Theoretical Total Phase Jitter against CNIR for Different Loop Bandwidths (Without Loop Aiding).
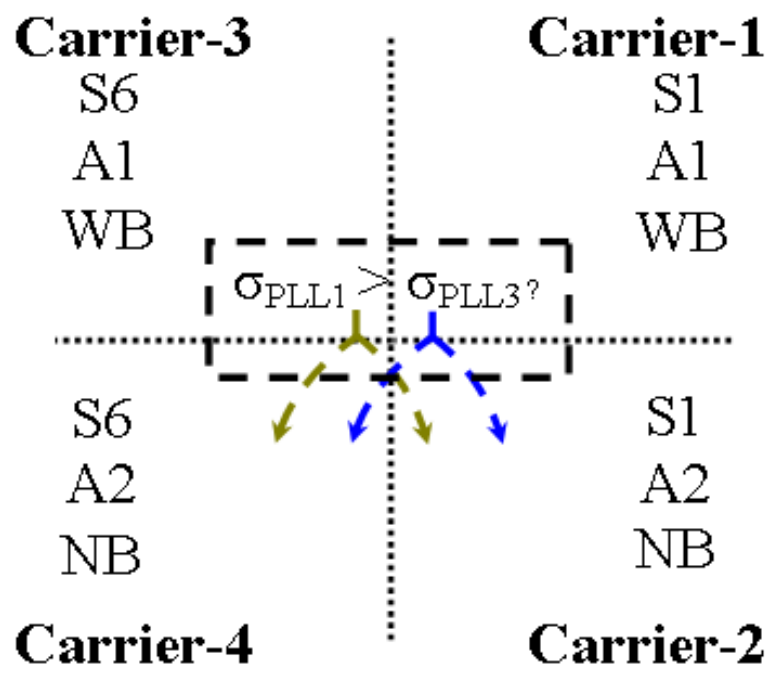
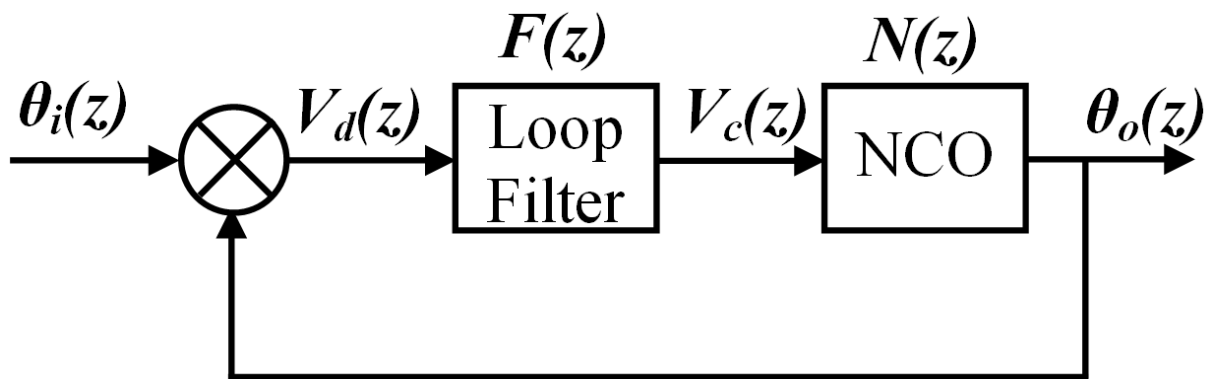Fig. 5.   Locata Carrier Chart
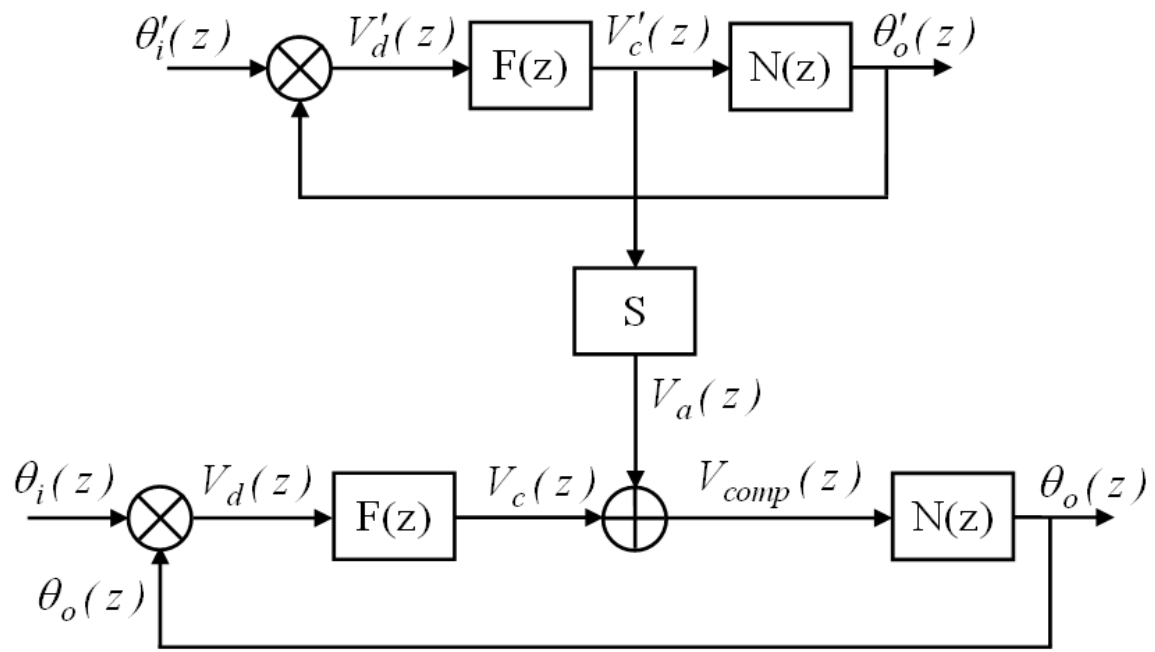
Fig. 6.   A Conceptual Un-aided PLL
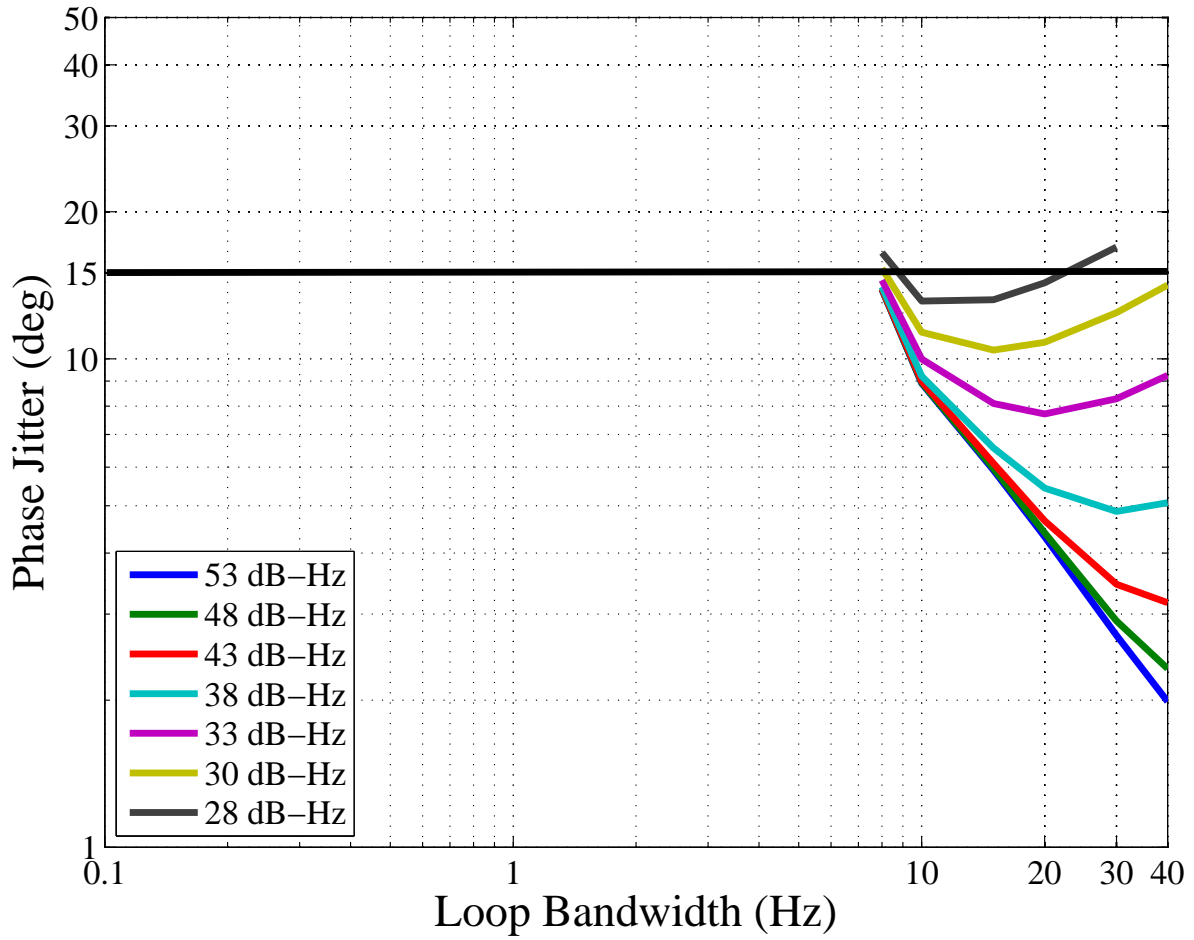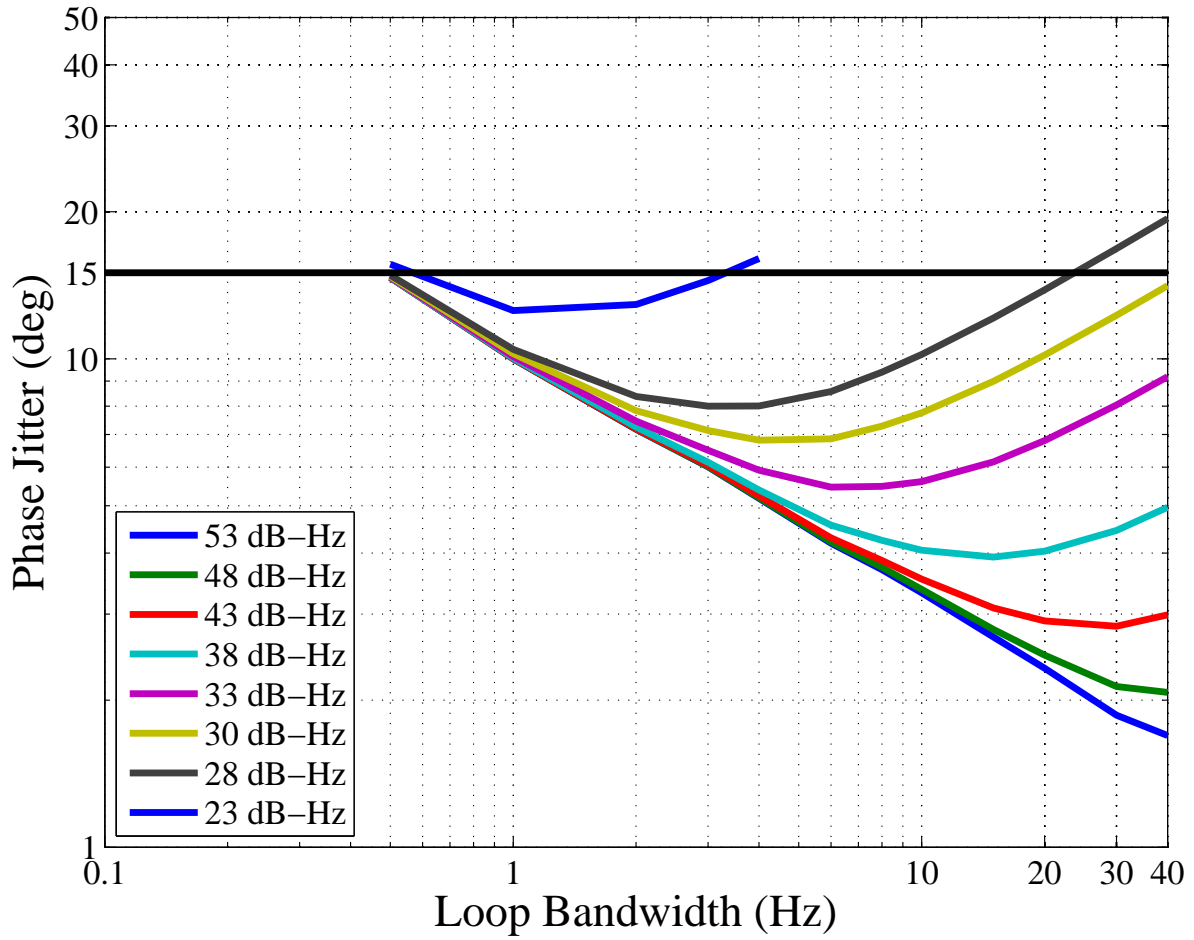
Fig. 7.   A Conceptual Inter-loop Aiding Design
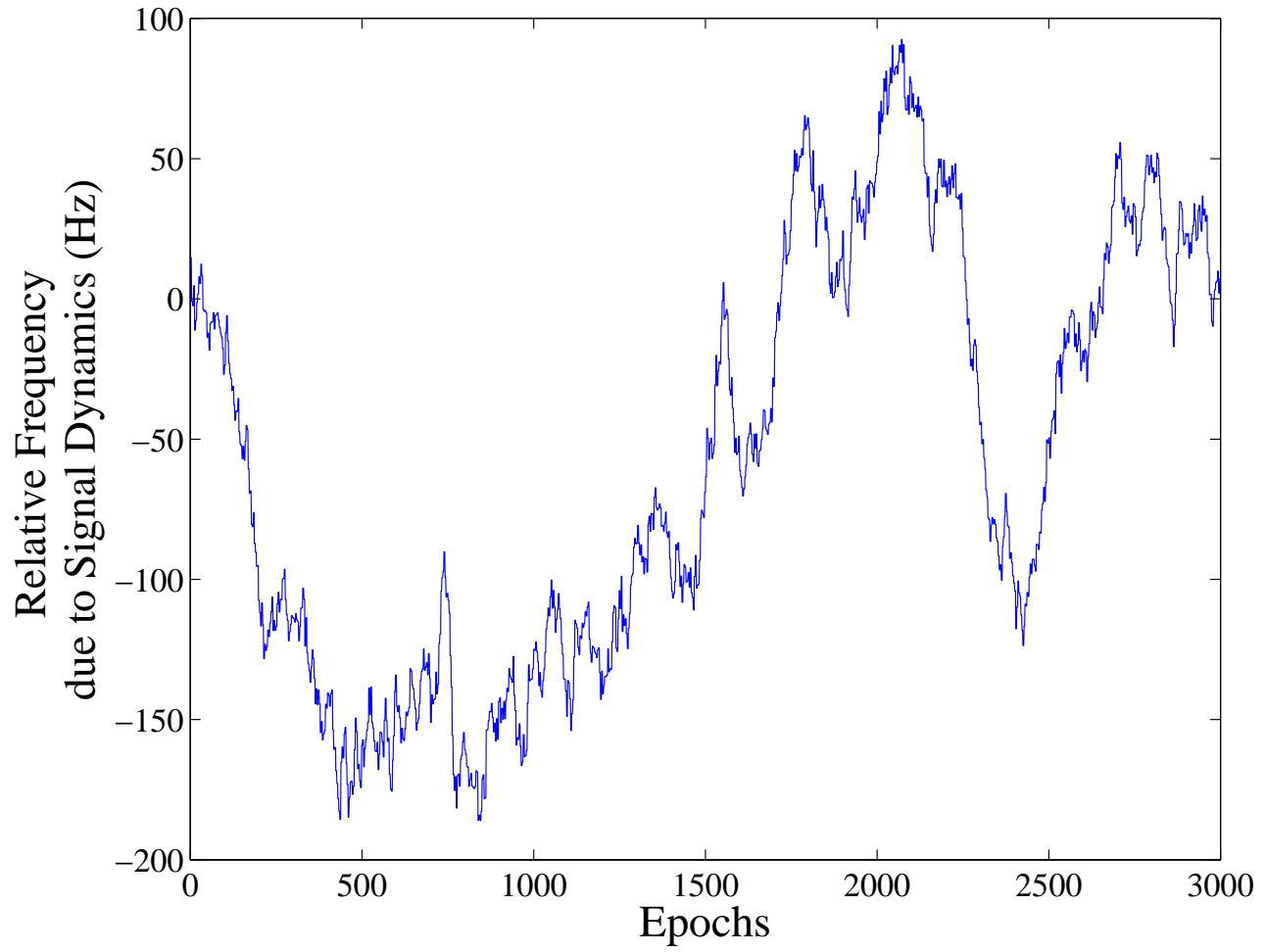
Fig. 8.   Relative Frequency due to Signal Dynamics

Fig. 9.   Phase Jitter against Loop Bandwidth for Different CNIR (Without Loop Aiding)
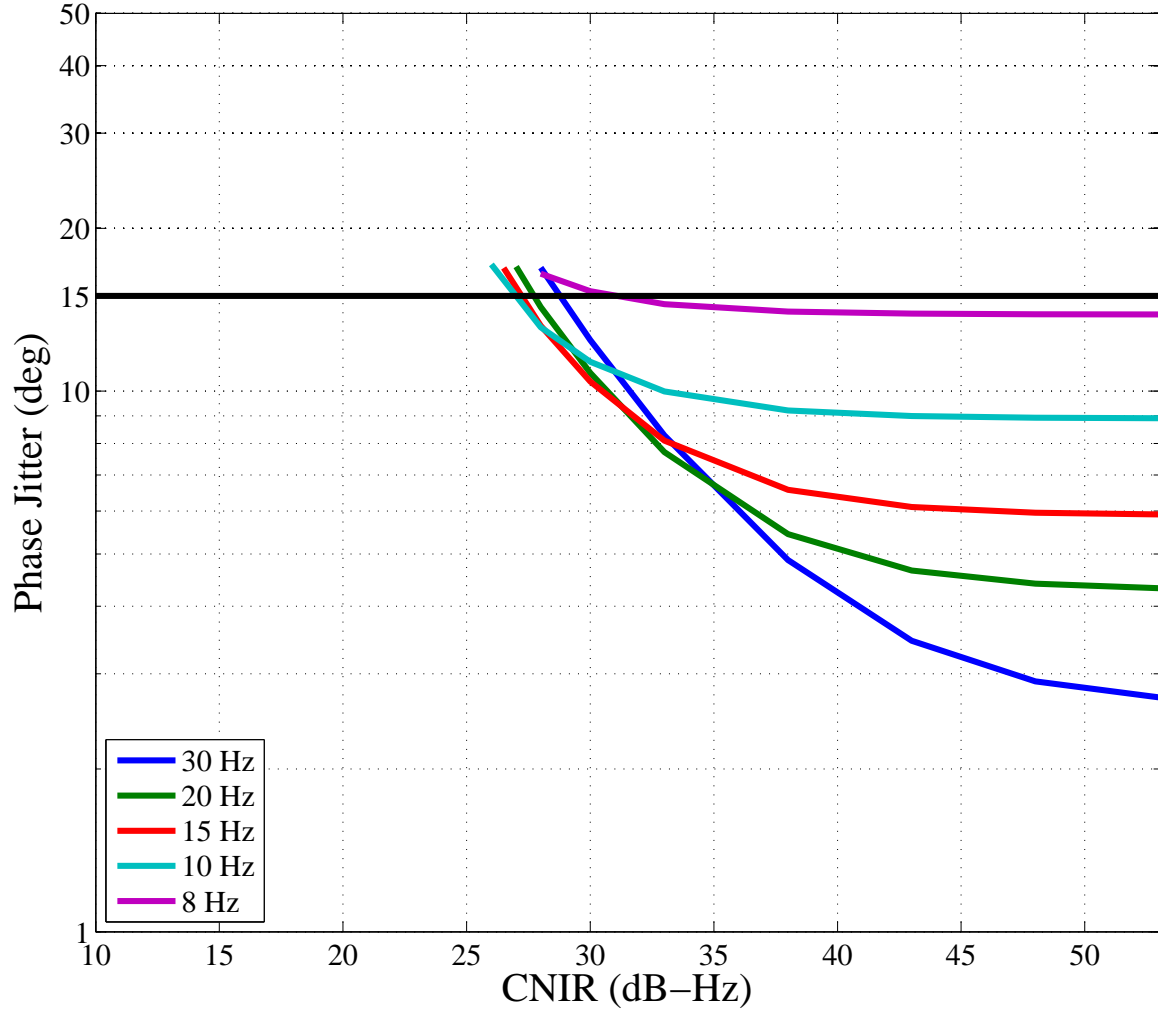
Fig. 10. Phase Jitter against CNIR for Different Loop Bandwidths (Without Loop Aiding)

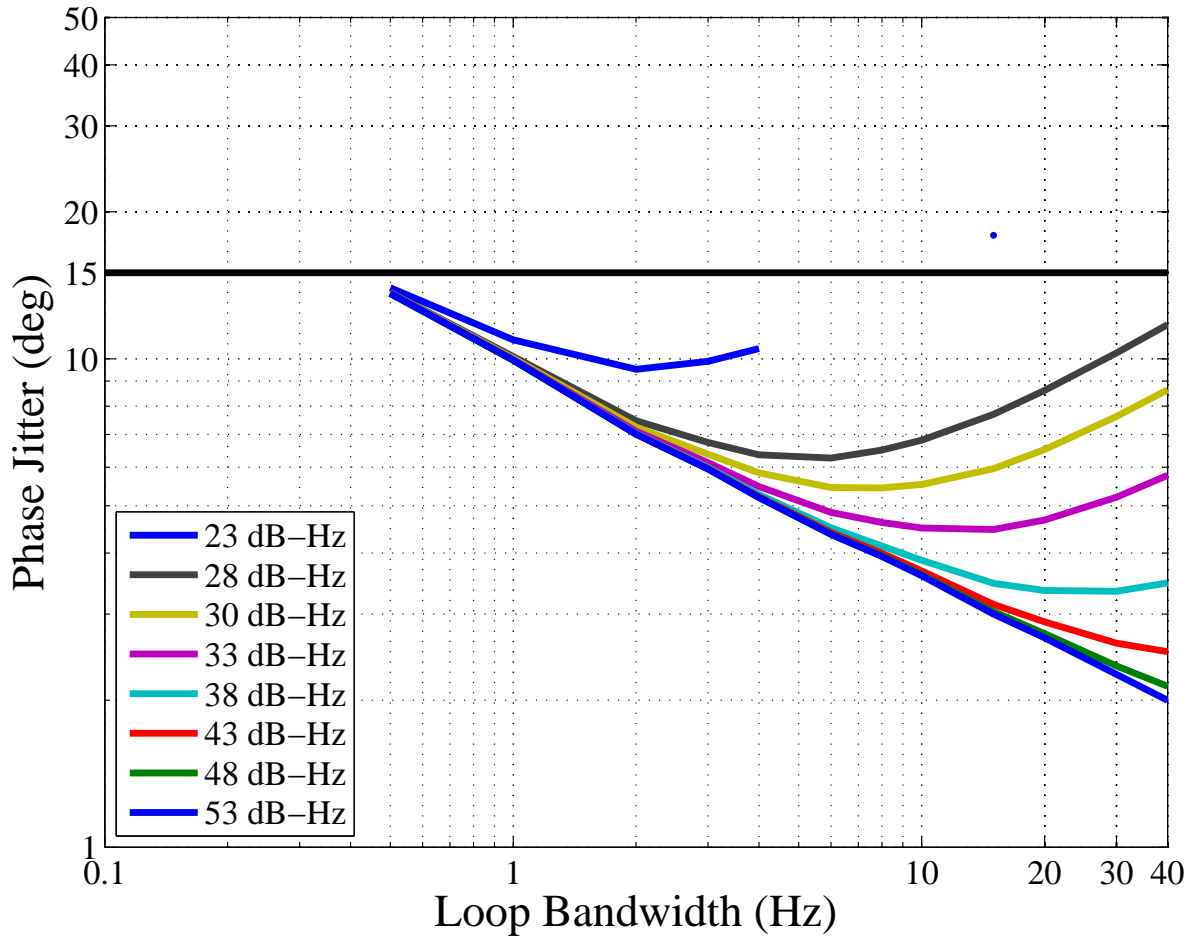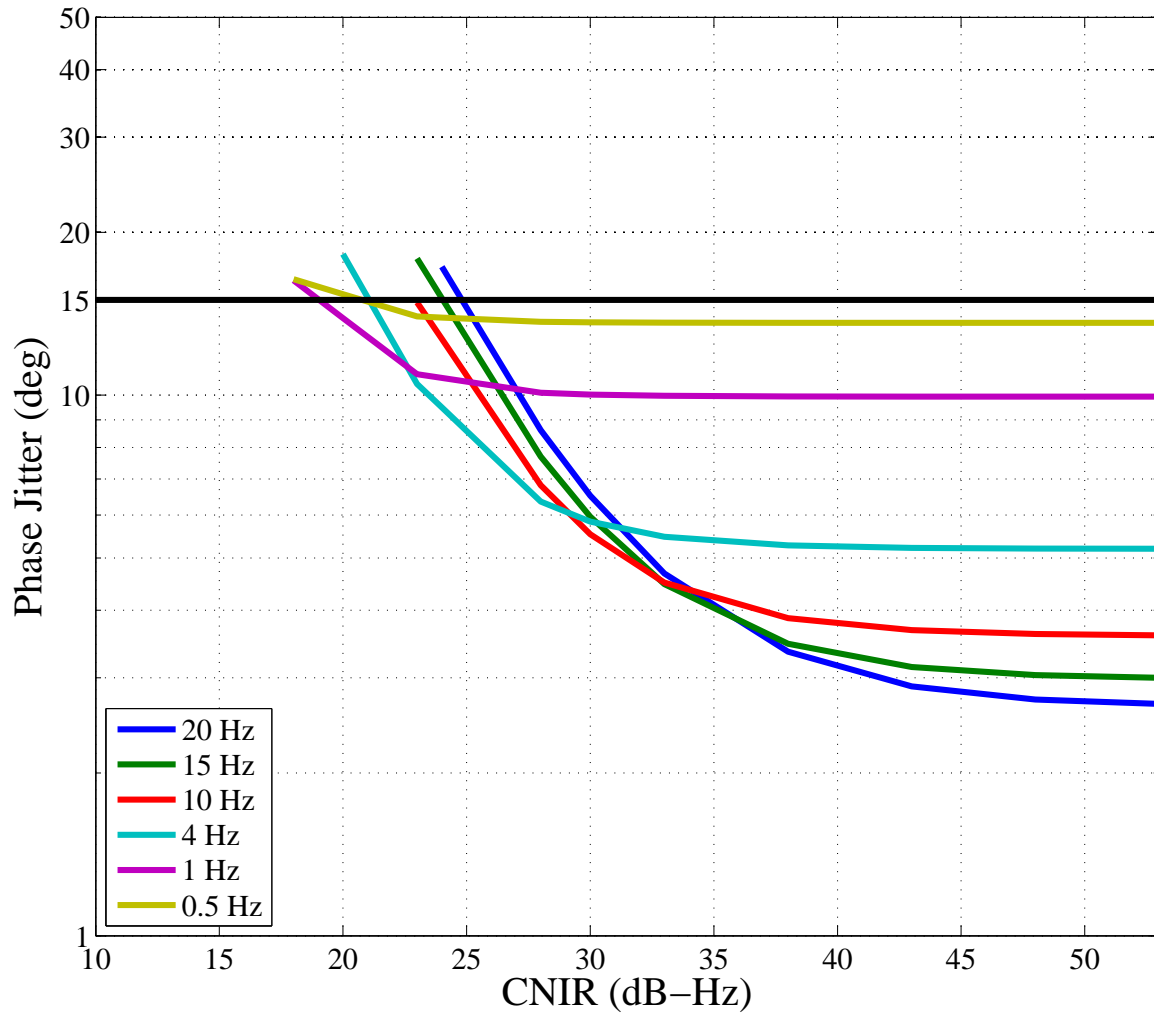Fig. 11.   Phase Jitter against Loop Bandwidth for Different CNIR (With Loop Aiding).
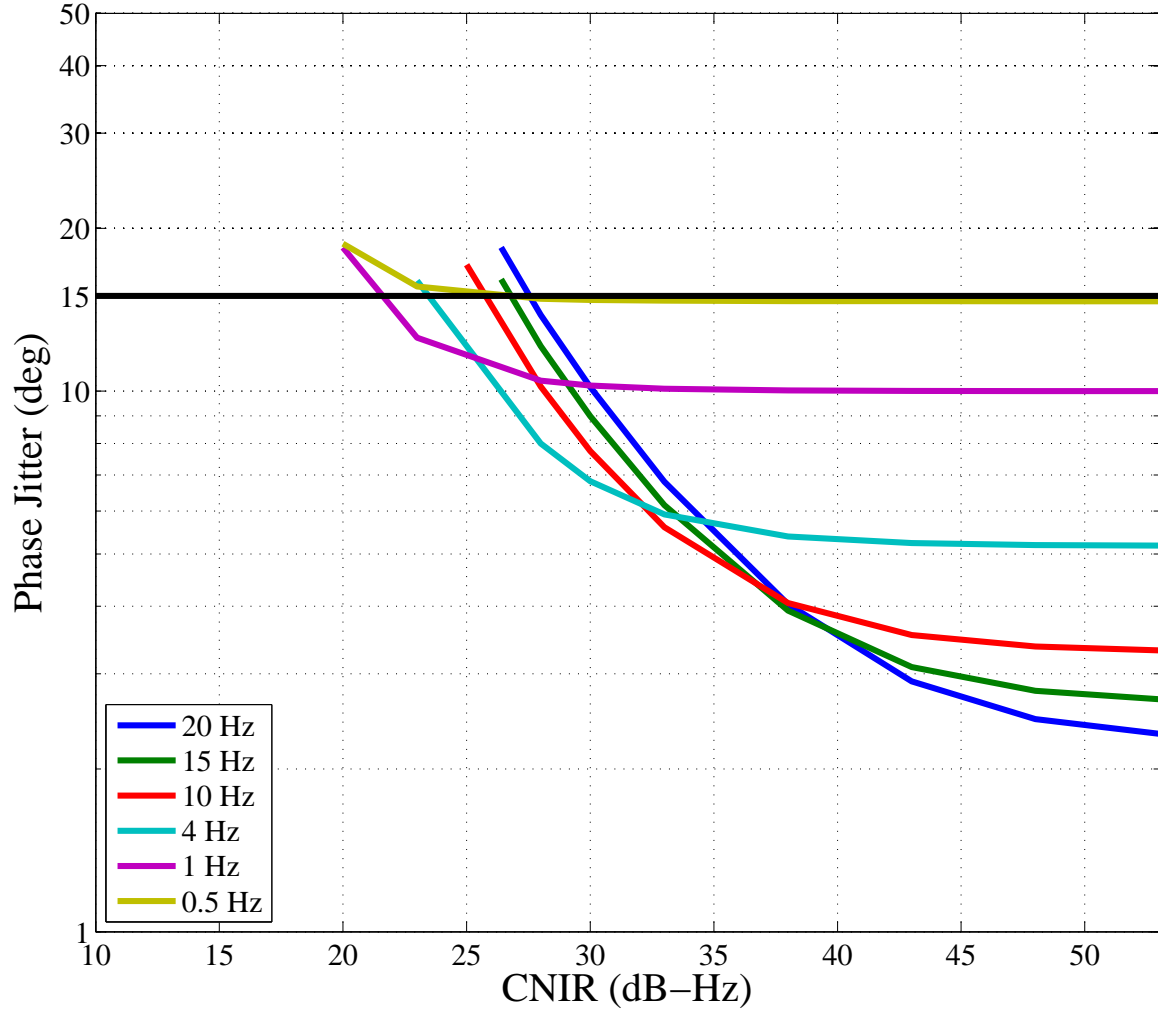
Fig. 12.   Phase Jitter against CNIR for Different Loop Bandwidths (With Loop Aiding).
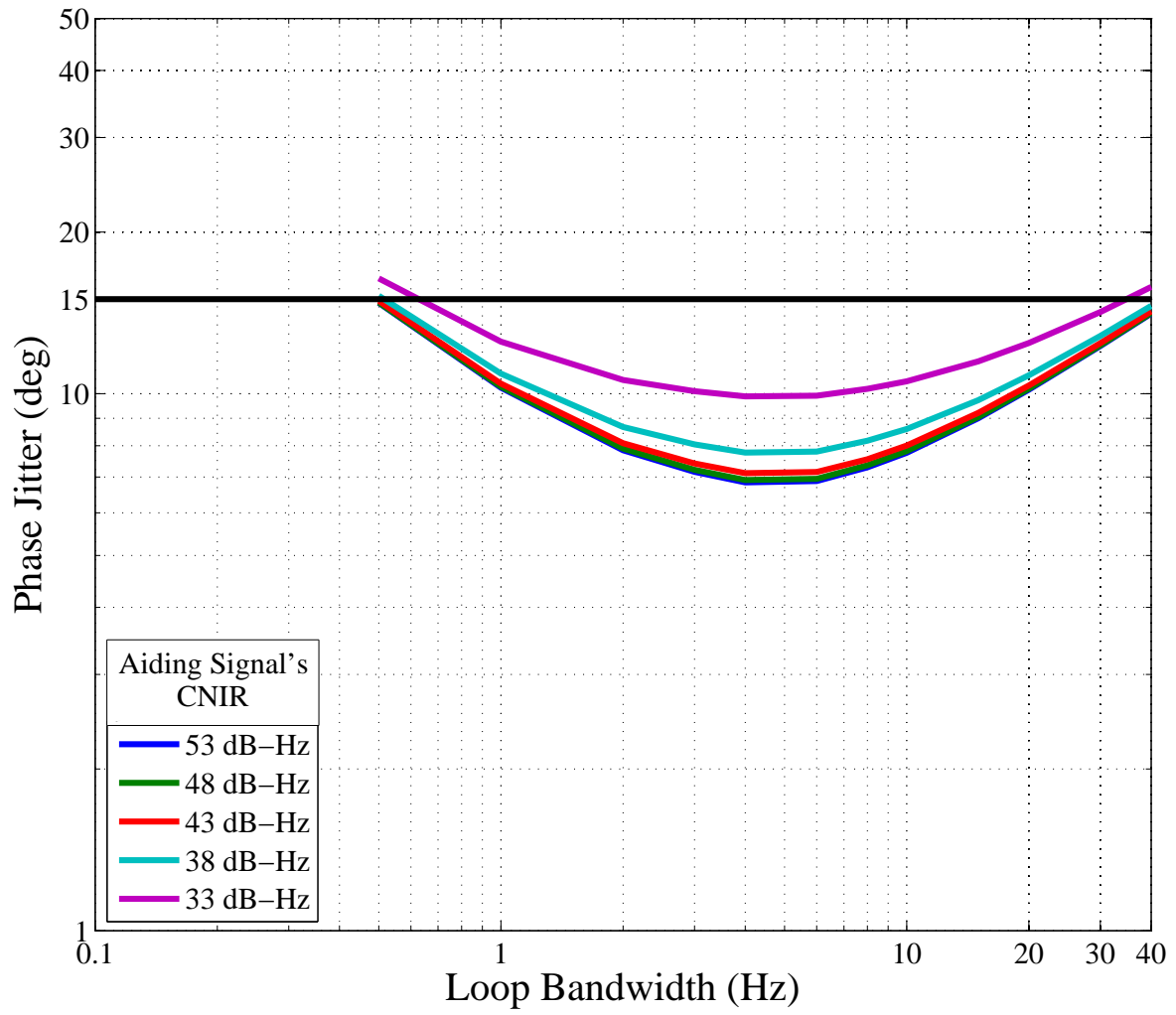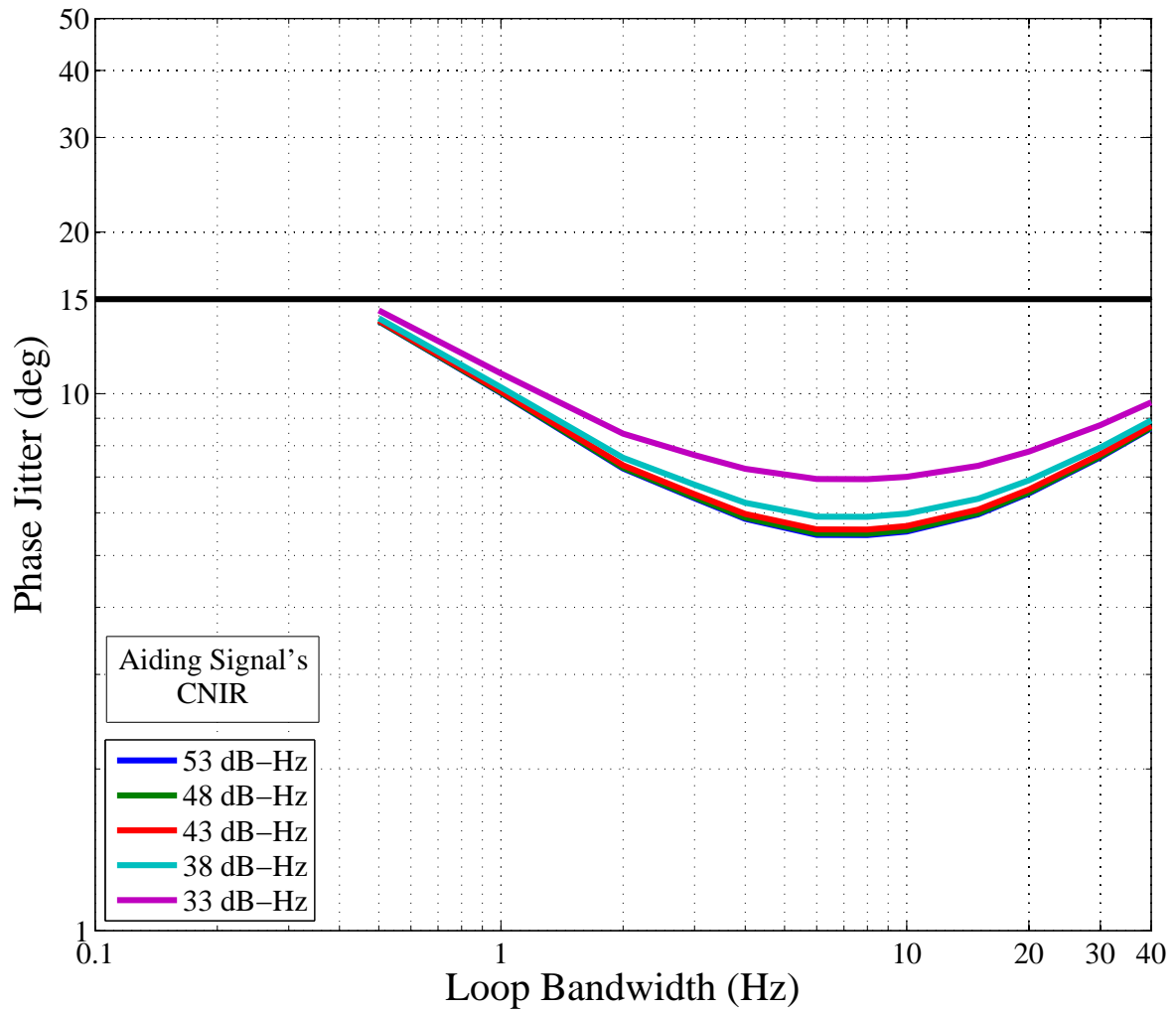
Fig. 13.   Phase Jitter against Aided Loop's Bandwidth for Different Aiding Signal's CNIR (With Loop Aiding). Interference affecting both aided and aiding loops.
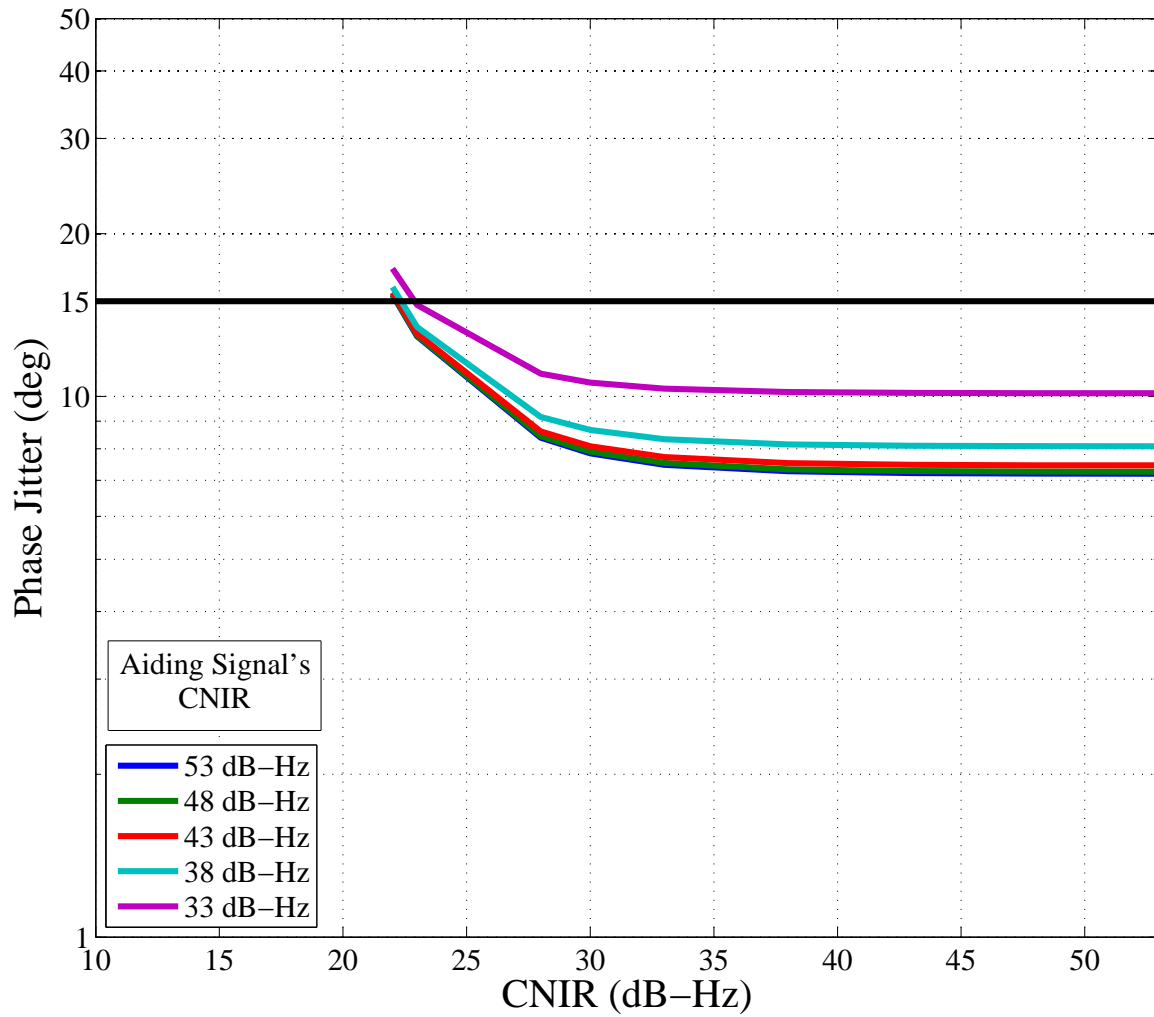
Fig. 14. Phase Jitter against Aided Signal's CNIR for Different Aiding Signal's CNIR (With Loop Aiding). Interference affecting both aided and aiding loops.
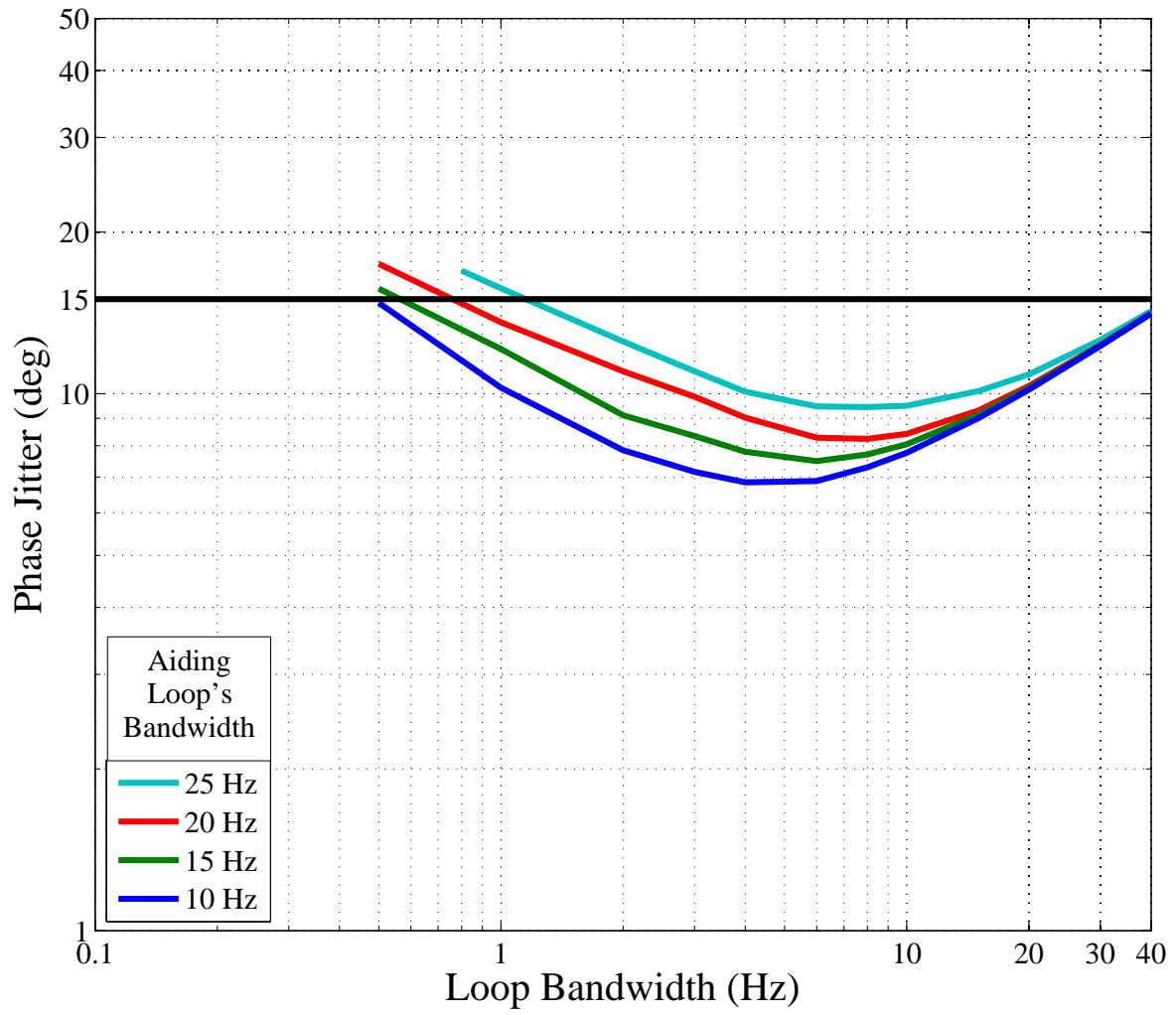
Fig. 15. Phase Jitter against Aided Loop's Bandwidth for Different Aiding Loop's Bandwidth (With Loop Aiding). Interference affecting both aided and aiding loops.
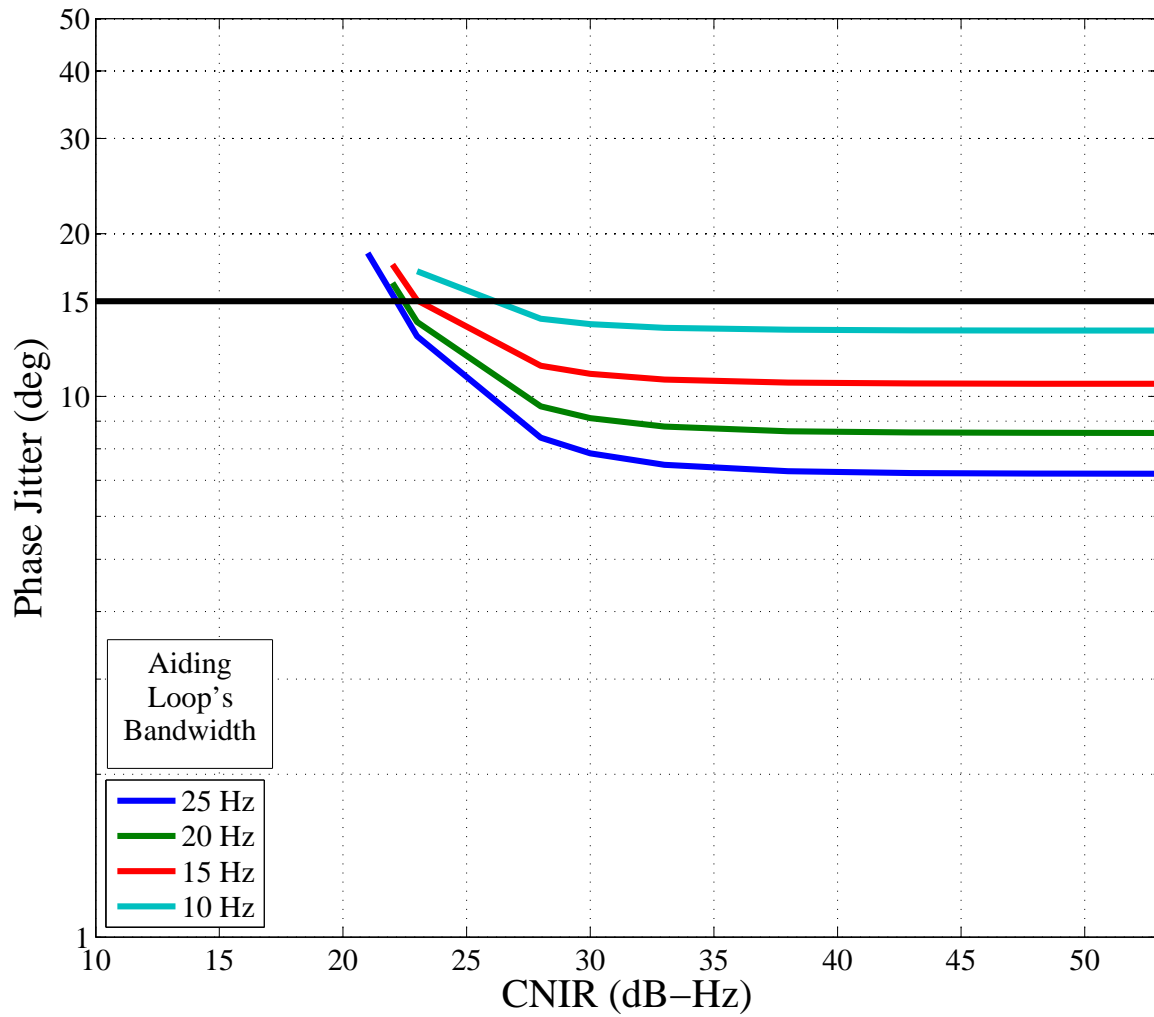
Fig. 16. Phase Jitter against Aided Signal's CNIR for Different Aiding Loop's Bandwidth (With Loop Aiding). Interference affecting both aided and aiding loops.
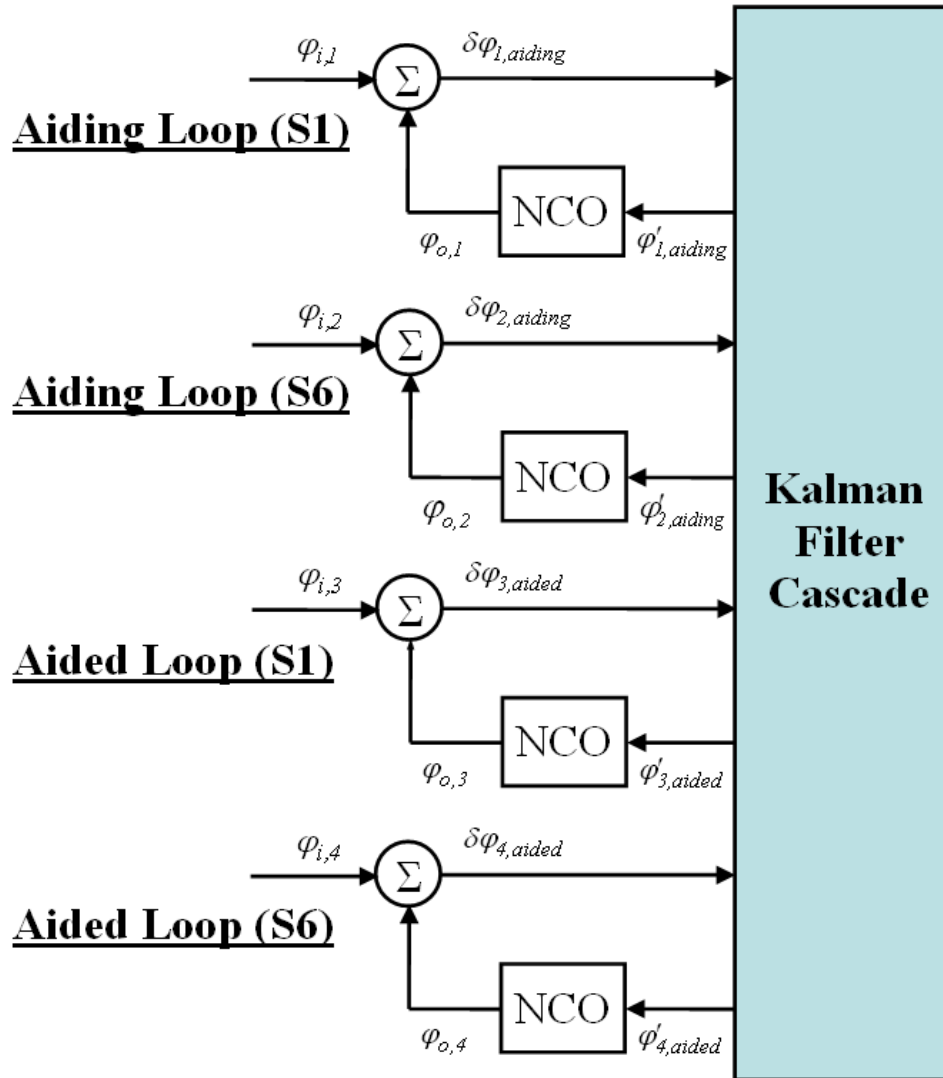
Fig. 17.   Phase Jitter against Aided Signal's CNIR for Different Aiding Loop's Bandwidth (With Loop Aiding). Interference affecting both aided and aiding loops.

Fig. 18.   Phase Jitter against Loop Bandwidth for Different CNIR (With AKF based Loop Aiding).

Fig. 19. Phase Jitter against CNIR for Different Loop Bandwidth (With AKF based Loop Aiding)

Fig. 20. Phase Jitter against Aided Loop's Bandwidth for Different Aiding Signal's CNIR (With AKF based Loop Aiding). Interference affecting both aided and aiding loops.
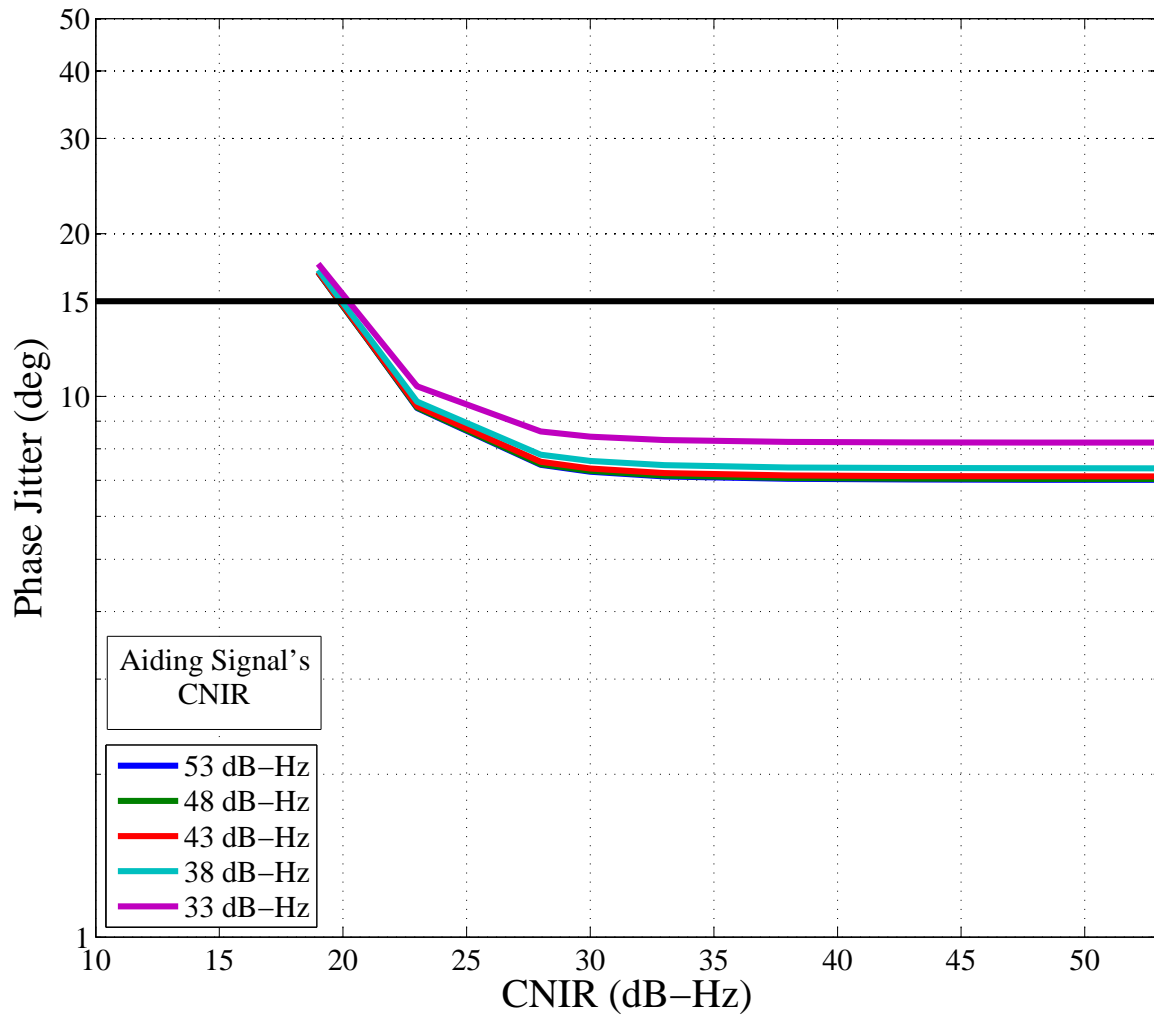
Fig. 21. Phase Jitter against Aided Signal's CNIR for Different Aiding Signal's CNIR (With AKF based Loop Aiding). Interference affecting both aided and aiding loops.
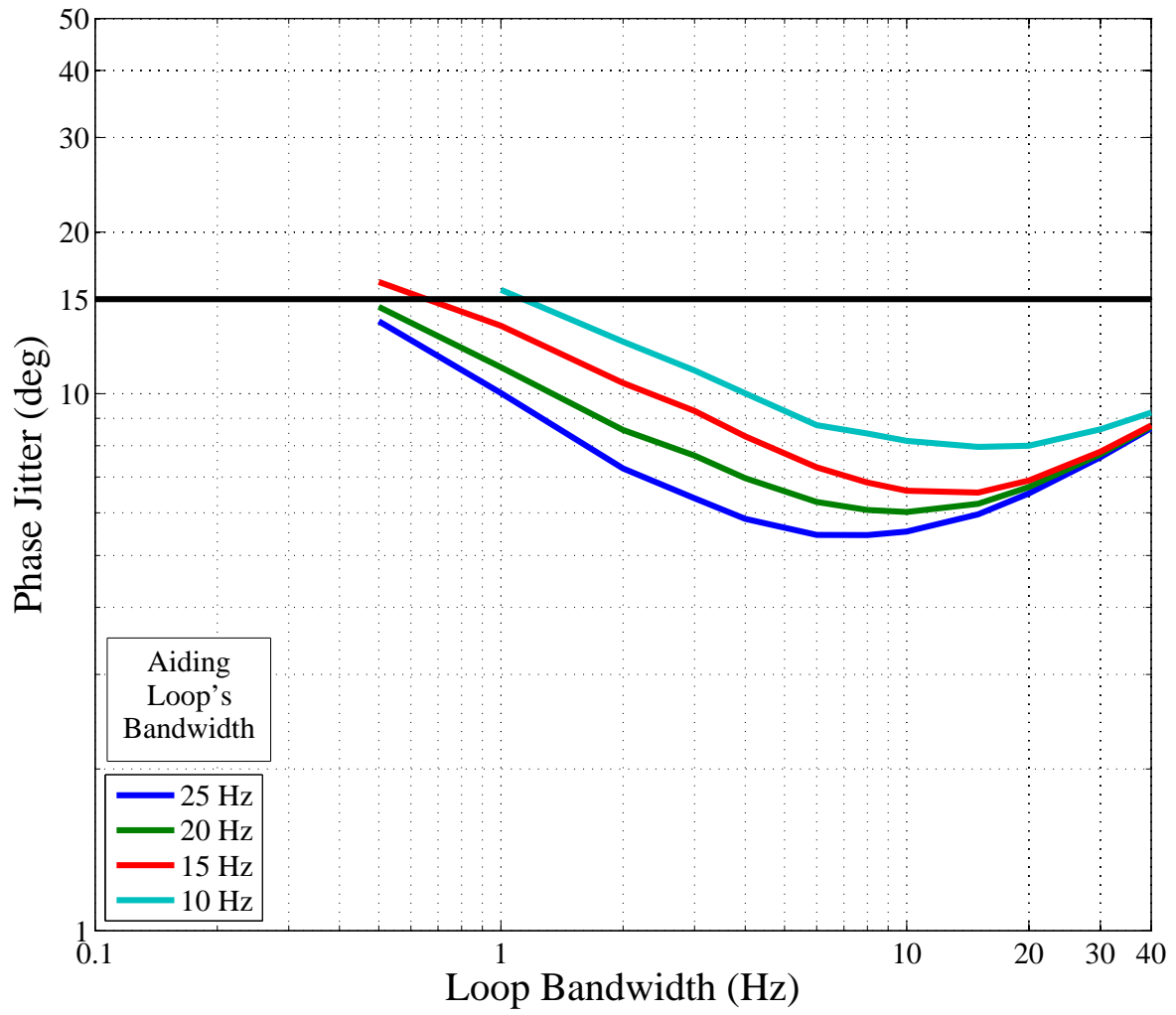
Fig. 22.   Phase Jitter against Aided Loop's Bandwidth for Different Aiding Loop's Bandwidth (With AKF based Loop Aiding). Interference affecting both aided and aiding loops.
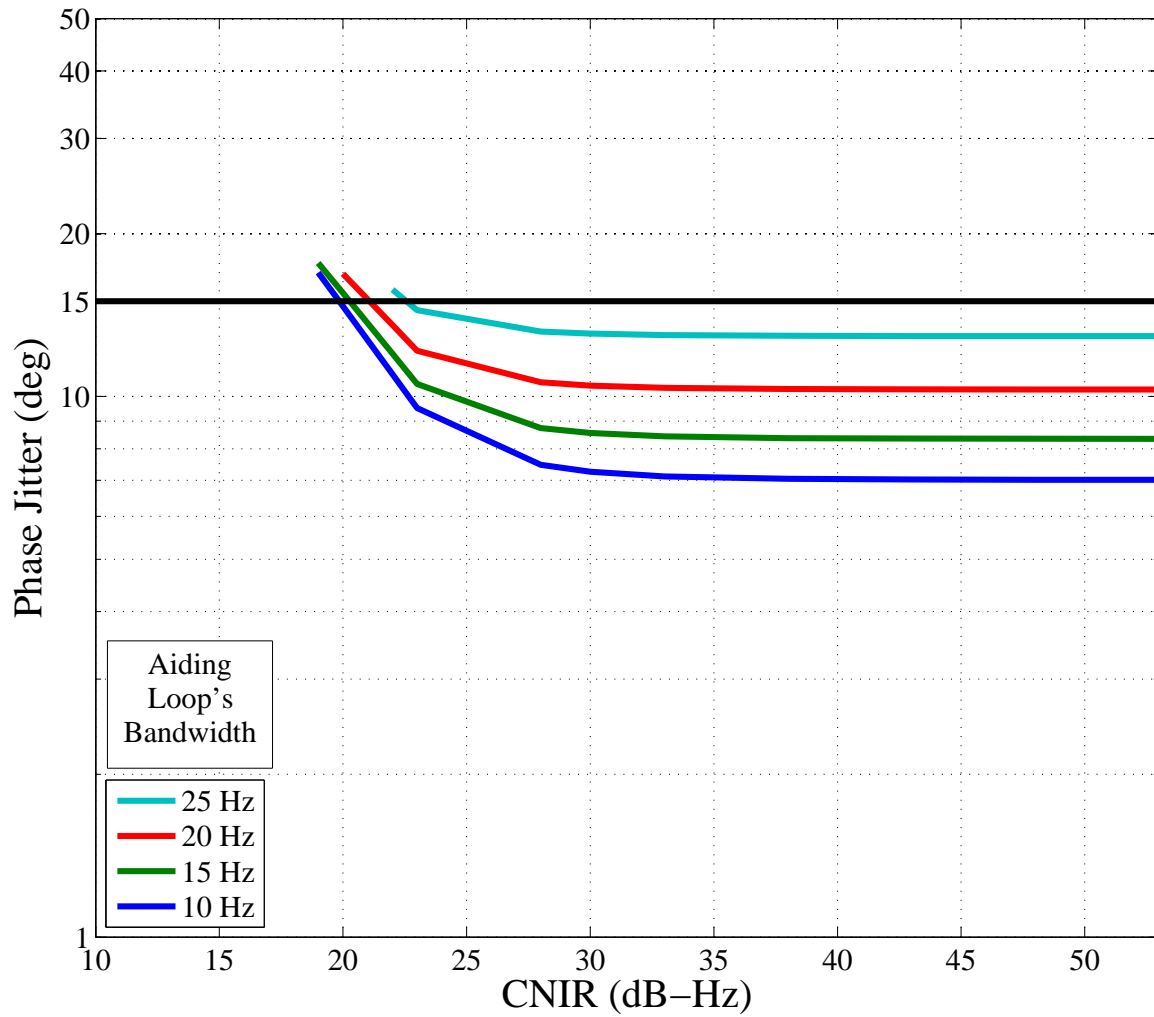
Fig. 23.   Phase Jitter against Aided Signal's CNIR for Different Aiding Loop's Bandwidth (With AKF based Loop Aiding). Interference affecting both aided and aiding loops.